C-type carbohydrate recognition domain. *J Biol Chem.* 2010;285:6390-6400.
21. Zweig MH, Campbell G. Receiver-operating characteristic (ROC) plots: a fundamental evaluation tool in clinical medicine. *Clin Chem.* 1993;39:561-577.
22. Inaguma S, Kasai K, Ikeda H. GLI1 facilitates the migration and invasion of pancreatic cancer cells through MUC5AC-mediated attenuation of E-cadherin [published online ahead of print October 25, 2010]. Oncogene. 2010.
23. Nakeeb A, Lipsett PA, Lillemoe KD, et al. Biliary carcinoembryonic antigen levels are a marker for cholangiocarcinoma. *Am J Surg* 171:147-152, 1996; discussion 152-143.
24. Ni XG, Bai XF, Mao YL, et al. The clinical value of serum CEA, CA19-9, and CA242 in the diagnosis and prognosis of pancreatic cancer. *Eur J Surg Oncol.* 2005;31:164-169.
25. Patel AH, Harnois DM, Klee GG, LaRusso NF, Gores GJ. The utility of CA 19-9 in the diagnoses of cholangiocarcinoma in patients without primary sclerosing cholangitis. *Am J Gastroenterol.* 2000;95:204-207.
26. Saito K, Fujii Y, Kawakami S, et al. Increased expression of sialyl-Lewis A correlates with poor survival in upper urinary tract urothelial cancer patients. *Anticancer Res.* 2003;23:3441-3446.
27. Uenishi T, Yamazaki O, Tanaka H, et al. Serum cytokeratin 19 fragment (CYFRA21-1) as a prognostic factor in intrahepatic cholangiocarcinoma. *Ann Surg Oncol.* 2008;15:583-589.
28. Watanabe H, Enjoji M, Nakashima M, et al. Clinical significance of serum RCAS1 levels detected by monoclonal antibody 22-1-1 in patients with cholangiocellular carcinoma. *J Hepatol.* 2003;39:559-563.
29. Del Favero G, Fabris C, Panucci A, et al. Carbohydrate antigen 19-9 (CA 19-9) and carcinoembryonic antigen (CEA) in pancreatic cancer. Role of age and liver dysfunction. *Bull Cancer.* 1986;73:251-255.
30. Del Favero G, Fabris C, Plebani M, et al. CA 19-9 and carcinoembryonic antigen in pancreatic cancer diagnosis. *Cancer.* 1986;57:1576-1579.

Identification of Four Isoforms of Aldolase B Down-regulated in Hepatocellular Carcinoma Tissues by Means of Two-dimensional Western Blotting

YUFENG WANG[1], YASUHIRO KURAMITSU[1], MOTONARI TAKASHIMA[1,2], YUICHIRO YOKOYAMA[1,3], NORIO IIZUKA[2], TAKAO TAMESA[2], ISAO SAKAIDA[3], MASAAKI OKA[2] and KAZUYUKI NAKAMURA[1]

Departments of [1]Biochemistry and Functional Proteomics, [2]Surgery and Clinical Science, and [3]Hepatology and Gastroenterology, Yamaguchi University Graduate School of Medicine, Ube, Japan

Abstract. *Background: Hepatocellular carcinoma (HCC) is one of the most lethal diseases, and one of the major causes of death in Japan. Our previous research of proteomics for cancerous and paired non-cancerous tissues from patients with HCC with hepatitis C virus infection (HCV-HCC) by means of the combination of two-dimensional gel electrophoresis (2-DE) and liquid chromatography tandem mass spectrometry (LC-MS/MS) reported that four of numerous spots of weaker intensity in cancerous tissues than in paired non-cancerous tissues were identified as four isoforms of liver type aldolase (aldolase B). In the present study, two-dimensional (2-D) Western blot analysis demonstrated a significantly lower expression of four isoforms of aldolase B in cancerous than in non-cancerous tissues. Conclusion: Our finding of differences of expression aldolase B isoforms between cancerous and paired non-cancerous tissues for HCV-HCC may be useful for shedding light on some behaviors of aldolase B during hepatocellular carcinogenesis.*

Hepatocellular carcinoma (HCC) is one of the world's most lethal diseases (1). Chronic infection with hepatitis C virus (HCV) is the major cause of the rising incidence of HCC in many countries (1, 2). Eighty percent of deaths from HCC are related to HCV infection in Japan (3).

In recent years, with the development of study of the proteome in HCV-related HCC, there has been a great progress in diagnosis and pathogenesis of HCV-HCC. Heat-shock protein 70 family members were identified as biomarkers and play important roles in the pathogenesis of HCV-HCC (5). Proteomic profiling demonstrated that some metabolic enzymes were decreased in cancerous tissues from patients with HCV-HCC compared to paired non-cancerous tissues, such as enoyl-CoA hydratase, aldolase B and arginase 1 (6). Plenty of biomarkers that showed differential expression between cancerous and non-cancerous tissues were found in HCC, by proteomic technologies, and were classified by following HCC with distinct causes (7). Our recent proteomic study of HCV-HCC tissues showed eight proteins to be down-regulated in HCC tissues from over 50% of the patients, identified as aldolase B, tropomyosin beta-chain, ketohexokinase, enoyl-CoA hydratase, albumin, smoothelin, ferritin light chain, and arginase 1. In particular, aldolase B was identified as four spots on the two-dimensional electrophoresis (2-DE) gel.

In the present study, we investigated these four spots which were identified as aldolase B by means of 2-D Western blot analysis with anti-aldolase B antibody.

Materials and Methods

Sample preparation. Twenty-two pairs of cancerous and paired non-cancerous liver tissues were obtained from patients with HCV-HCC who had undergone surgical hepatectomy at the Department of Surgery II at Yamaguchi University Hospital. None of the patients received any preoperative therapy. Written informed consent was obtained from all patients prior to surgery. The study protocol was approved by the Institutional Review Board for Human Use of the Yamaguchi University School of Medicine. Specimens were resuspended and homogenized in lysis buffer (1% NP-40, 1mM sodium vanadate, 1 mM PMSF, 10 mM NaF, 10 mM EDTA, 50 mM Tris, 165 mM NaCl, 10 μg/ml leupeptin, and 10 μg/ml aprotinin) on ice (8). Suspensions were incubated for 2 h at 4°C, and centrifuged at 15 000 × *g* for 30 min at 4°C, then the supernatants were extracted and stored at –80°C until use.

Correspondence to: Yasuhiro Kuramitsu, MD, Ph.D., Department of Biochemistry and Functional Proteomics, Yamaguchi University Graduate School of Medicine, 1-1-1 Minami-Kogushi, Ube, Yamaguchi 755-8505, Japan. Tel: +81 836222213, Fax: +81 836222212, e-mail: climates@yamaguchi-u.ac.jp

Key Words: Two-dimensional gel electrophoresis, LC-MS/MS, 2-D Western blotting, hepatocellular carcinoma, aldolase B.

0258-851X/2011 $2.00+.40

2-DE. Eighty micrograms of protein was used for each electrophoretic run. Sample was mixed with 200 μl of rehydration buffer [8 M urea, 2% 3-(3-cholamidopropyl) dimethylammonio-1-propanesulfonate (CHAPS), 0.01% bromophenol blue, 1.2% Destreak reagent (GE Healthcare, Bukinghamshire, UK) and 0.5% IPG buffer (GE Healthcare). Rehydration was performed in an IPGphor 3 Isolelectric Focusing (IEF) unit (GE Healthcare) on 11 cm, immobilized pH 3-10 linear gradient IPG strips (Bio-Rad, Hercules, CA, USA) at 50 μA/strip. IEF was performed as following conditions: rehydration for 10 h; 0 to 500 V for 4 h; 500 to 1000 V for 1 h; 1000 to 8000 V for 4 h; 8000 V for 20 min; and the final phase of 500 V from 20000 to 30000 Vh. The strips were subsequently equilibrated in equilibration buffer 1 [6 M urea, 0.5 M Tris-HCl pH 8.8, 30% glycerol, 2% sodium lauryl sulfate (SDS), 2% 2-mercaptoethanol (2-ME)] for 10 min and then continued in equilibration buffer 2 (6 M urea, 0.5 M Tris-HCl pH 8.8, 30% glycerol, 2% SDS, 2.5% iodoacetoamide) for another 10 min. The strips were then transferred onto gels and run at 200 V (9).

Image analysis and spot picking. The SDS-PAGE gels were incubated with solution containing 40% ethanol and 10% acetic acid for 2.5 h. The gels were then stained with a fluorescent gel staining, Flamingo™ Fluorescent Gel Stain (Bio-Rad) overnight (10). The gels were scanned by using a ProEXPRESS 2 D Proteomic Imaging System (PerkinElmer, Waltham, MA, USA) and then analyzed by using Progenesis Samespots software (Nonlinear, Newcastle, upon Tyne, UK). After image analysis, the gels were stained with See Pico™ (Benebiosis, Seoul, Korea) overnight (11). Protein spots were picked out from each gel and immersed in 70 μl ultra-pure water.

In-gel digestion. The See Pico™ dye was removed by washing three times in 60% methanol, 0.05 M ammonium bicarbonate, and 0.005 M DL-dithiothreitol (DTT) for 15 min. The sample in the gel piece was reduced twice in 50% methanol, 0.05 M ammonium bicarbonate, and 0.005 M DTT for 10 min. The gel pieces were dehydrated twice in 100% acetonitrile (ACN) for 30 min and incubated with an in-gel digestion reagent containing 10 μg/ml sequencing-grade-modified trypsin (Promega, Madison, WI, USA) in 30% ACN, 0.05 M ammonium bicarbonate, and 0.005 M DTT at 30°C overnight. The samples were lyophilized overnight with the use of Labconco Lyph-lock 1L Model 77400 (Labconco, Kansas, MO, USA) (12).

LC-MS/MS. The lyophilized samples were dissolved in 30 μl formic acid and centrifuged at 15,000 × *g* for 5 min. Peptide sequencing of identified protein spots was performed by using an Agilent 1100 LC-MSD Trap XCT (Agilent Technologies, Palo Alto, CA, USA). Fifteen microliters of each sample was injected and separated on a Zorbax 300SB-C18 column (75 μm, 150 mm; Agilent Technologies). The Agilent 1100 capillary pump worked with the following conditions: solvent A, 0.1% formic acid; solvent B, ACN in 0.1% formic acid. Column flow, 0.3 μl/min; primary flow 300 μl/min. Gradient, 0-5 min 2% B, 60 min 60% B. Stop time: 60 min. Proteins were identified in an Agilent Spectrum Mill MS proteomics workbench against the Swiss-Prot protein database search engine (http://kr.expasy.org/sprot/) and MASCOT MS/MS Ions Search engine (http//www.matrixscience.com/search_form_select.html). Standard for induction of candidate proteins were set as follows: filter by protein score >10.0, and filter peptide by score >8. The Spectrum Mill workbench searched MS/MS spectra using an MS/MS ion search (13, 14).

2-D Western blot analysis. Four pairs of samples were separated on 2-DE gels and then transfer onto polyvinylidene fluoride (PVDF) membranes (Immobilon; Millipore, Bedford, MA, USA) at 90 mA for 78 min. The membranes were blocked overnigh with Tris-buffered saline (TBS) containing 5% milk at 4°C (8). Membranes were incubated with the primary antibody against aldolase B (Anti-aldolase B goat polyclonal antibody 1:100; Santa Cruz Biotechnology, Santa Cruz, CA, USA). Membranes were incubated with the secondary antibody conjugated with horseradish peroxidase (1:10,000) for 1 h at room temperature after washing three times with TBS containing Tween-20 and once with TBS. Membranes were then treated with a chemiluminescent reagent (ImmunoStar Long Detection, Wako, Osaka, Japan) and imaged using an Image Reader LAS-1000 Pro (Fujifilm Corporation, Tokyo, Japan).

Results

Detection of protein spots on 2-DE gels. Twenty-two pairs of cancerous and paired non-cancerous tissues from patients with HCV-HCC were analyzed by 2-DE. Hundreds of protein spots were visualized on 2-DE gels. Four spots of down-regulated proteins (spots 1-4) were revealed on 2-DE gels of cancerous and paired non-cancerous tissues with a >1.5-fold difference in intensity (Figure 1).

Identification of proteins by LC-MS/MS. The four spots were digested and analyzed by MS. Each spot provided a good spectrum of amino acids by analysis with LC-MS/MS. Aldolase B isoforms (spots 1-4) showing underexpression in cancerous tissues compared to paired non-cancerous tissues on 2-DE gels were identified and listed in Table I. MS and MS/MS spectra of trypsin-digested spot 2 are shown in Figure 2.

2-D Western blot analysis of aldolase B isoforms. Four pairs of cancerous and paired non-cancerous tissues from patients with HCV-HCC were analyzed by 2-D Western blot analysis with specific anti-aldolase B antibody. The spots were confirmed as four aldolase B isoforms (Figure 3A). The differential intensities of protein spots were quantified (Figure 3B) and the four proteins were found to be significantly down-regulated ($p<0.05$) in cancerous tissues compared to non-cancerous tissues.

Discussion

Fructose-1,6-(*bis*)phosphase aldolase exists as three isozymes with different tissue distributions: aldolase A (muscle and red blood cell), aldolase B (liver, kidney and small intestine), and aldolase C (brain and neuronal tissues) (15). Aldolase B catalyzes the reversible cleavage of fructose-1,6-(*bis*) phosphate (FBP) and fructose-1-phosphate (F1P) to dihydroxyacetone phosphate and either glyceraldehyde-3-phosphate or glyceraldehyde, respectively (16). Not only that, but aldolase B is also involved in the

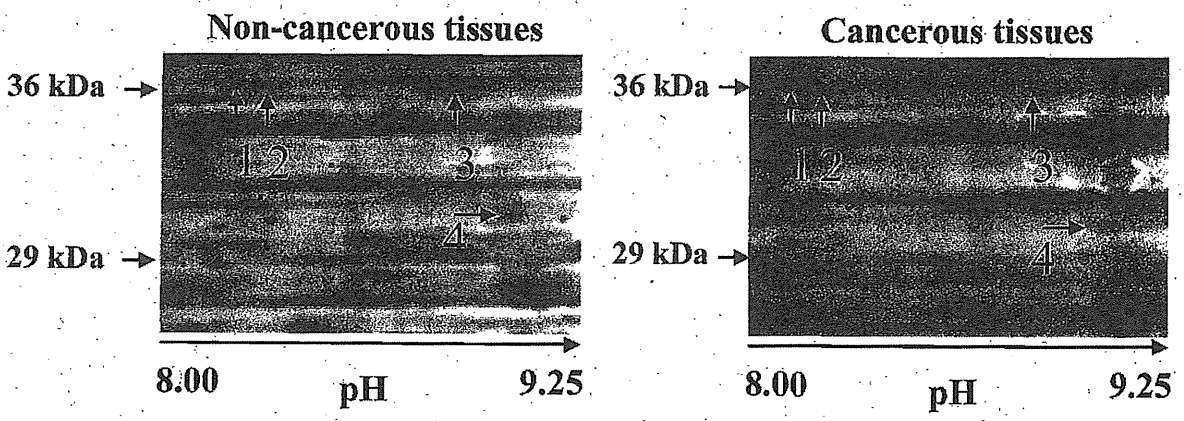

Figure 1. *Down-regulated expression of four proteins in HCC. Four protein spots (numbered 1-4) were found to be differentially expressed on 2-DE gels of proteins from samples of cancerous and paired non-cancerous tissues.*

Table I. *Identification of the protein spots in cancerous tissues.*

Spot	Distinct peptides	MS/MS search score	Coverage (%)	Frequency	Mass (Da)/pI	Accession no.	Protein
1	3	42.13	14%	18/22	39473.2/8.00	P05062	Aldolase B
2	3	40.43	8%	17/22	39473.2/8.00	P05062	Aldolase B
3	5	70.08	16%	18/22	39473.2/8.00	P05062	Aldolase B
4	4	49.51	22%	18/22	39473.2/8.00	P05062	Aldolase B

two opposite metabolic pathways, glycolysis and gluconeogenesis (17). The mRNA of aldolase B was down-regulated in HCC patients and its protein expression was shown to be down-regulated in cancerous tissue compared with surrounding non-cancerous tissues in HCV-HCC (6, 18). However, aldolase A was up-regulated in hepatoma cell lines and cancerous tissues from patients with HCC compared to surrounding non-cancerous tissues (19, 20). Because aldolase A seems to be customized for a glycolytic role, while aldolase B may function mainly in glyconeogenesis (17), this kind of displacement between aldolase A and B in cancerous tissues in HCC may be involved in the imbalance of glycometabolism in patients' liver tissues (21, 22), leading to tumor progression for HCC.

In this study, aldolase B was identified as existing in four isoforms in liver tissues from patients with HCV-HCC, and 2-D Western blotting demonstrated that protein expression of the four isoforms of aldolase B was significantly down-regulated in cancerous compared to paired non-cancerous tissues. However, the relationships between functional mechanisms and post-translational modifications (PTMs) of aldolase B isoforms in liver tissue remain unclear. The cognate aldolase B mRNA encodes a 364 amino acid protein with a molecular weight of 39.3 kDa (23). It has strictly conserved residues in the active site consisting of Asp33, Arg42, Lys107, Lys146, Glu187, Ser271, Arg303 and Lys229 (24). Arg303 and Arg42 residues are involved in one of the two alternate C6-binding sites (25). Lys146, a residue required for carbon–carbon bond cleavage, is able to perturb the pKa values of important residues in catalysis, such as the Schiff-base Lys229 and general acid/base catalyst Asp33, towards neutrality (24, 26). The subtle changes in position of Lys146 may alter the reactivity of these essential residues (27). Lys146 and Glu187 are directly bound to the product of the catalytic reaction (DHAP) (28). Presumably, aldolase B isoforms in liver tissue may be associated with the PTMs of these functional positions. Despite that less than 22% of a full length sequence of aldolase B was analyzed by using an MS system (shown in Table I), no interesting differences of PTMs among four isoforms of aldolase B were found. Therefore, in order to understand the effects of aldolase B isoforms on occurrence and development of HCV-HCC, the key PTMs among them should be identified in further study. Accordingly, it is necessary to improve quantity and purity of protein samples for analysis by LC-MS/MS. In addition, aldolase not only plays an essential role in glycometabolism, but also interacts with macromolecules unrelated to the glycometabolic pathway, such as F-actin (29), cell surface

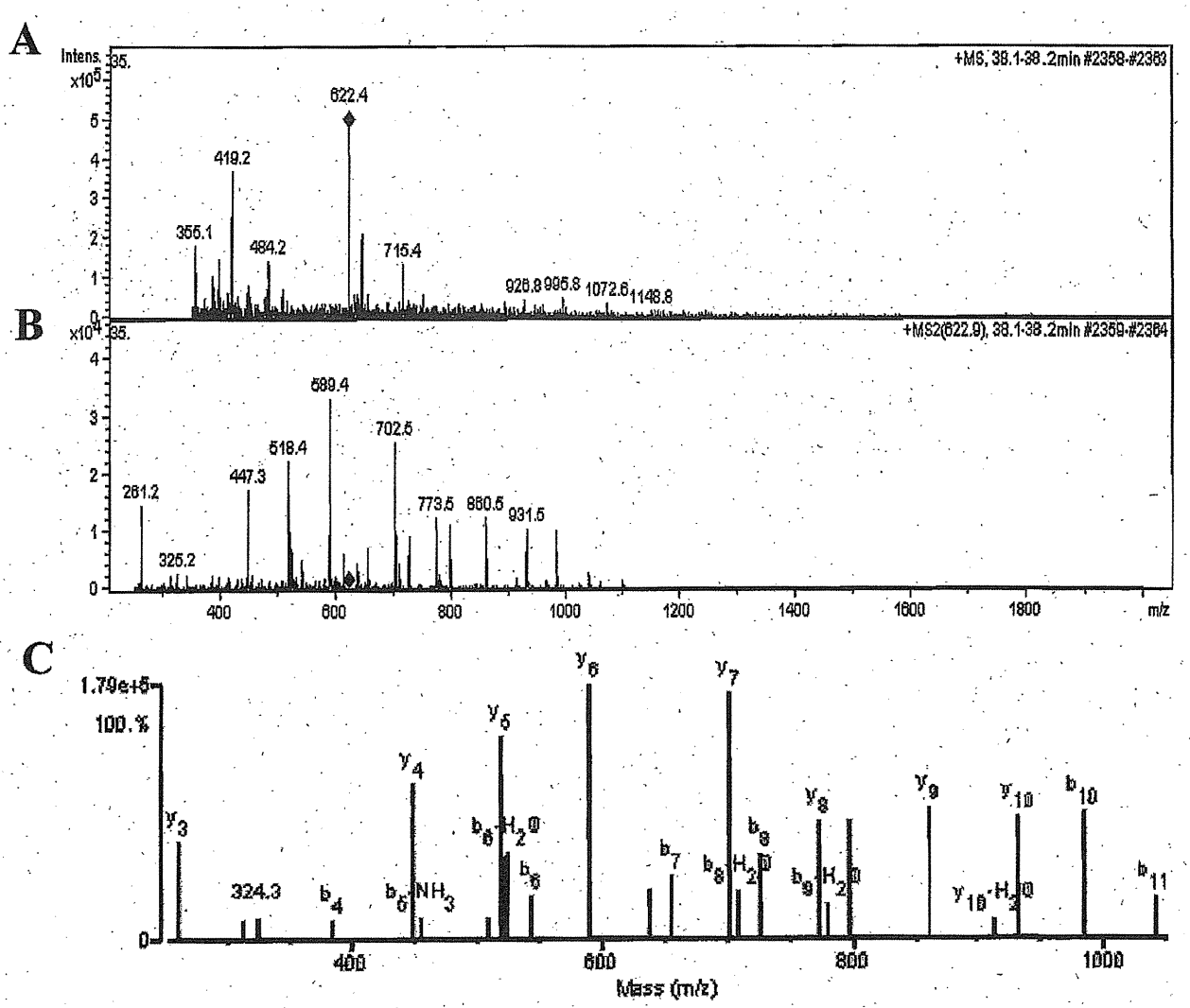

Figure 2. *MS and MS/MS spectra of trypsin-digested spot 2. A: LC-MS spectra of trypsin-digested of spot 2; aldolase B precursor ion m/z is 622.4. B and C: LC-MS/MS spectrum of a precursor ion with m/z 622.4 marked by a diamond in (A). The MS/MS spectrum identifies the partial tryptic peptide [R]ALQASALAAWGGK[A] from aldolase B processed with a spectrum Mill workbench.*

adhesins (30), RNA (31), tubulin (32) and liver cytoskeleton (33). Therefore aldolase B isoforms might be involved in tumor progression in a glycometabolism-independent manner.

Conclusion

Proteomic technology, such as 2-DE and MS analysis, has been widely employed in the research of discovery of biomarkers in diseases, especially in cancer. Differences of expression of aldolase B isoforms between cancerous and paired non-cancerous tissues were identified in HCV-HCC by those of technologies in current study. Simultaneously, four isoforms of aldolase B were identified and quantified by performing 2-D Western blotting and statistical analysis. These findings may be useful for shedding light on some behaviors of aldolase B during hepatocellular carcinogenesis. In order to assess the function of aldolase B in HCV-HCC, we will focus on finding the key PTMs among four isoforms of aldolase B in further study.

Acknowledgements

This work was supported in part by Grants-in-Aid from the Ministry of Health, Labour and Welfare of Japan (No. H20-Bio-005 to Kazuyuki Nakamura).

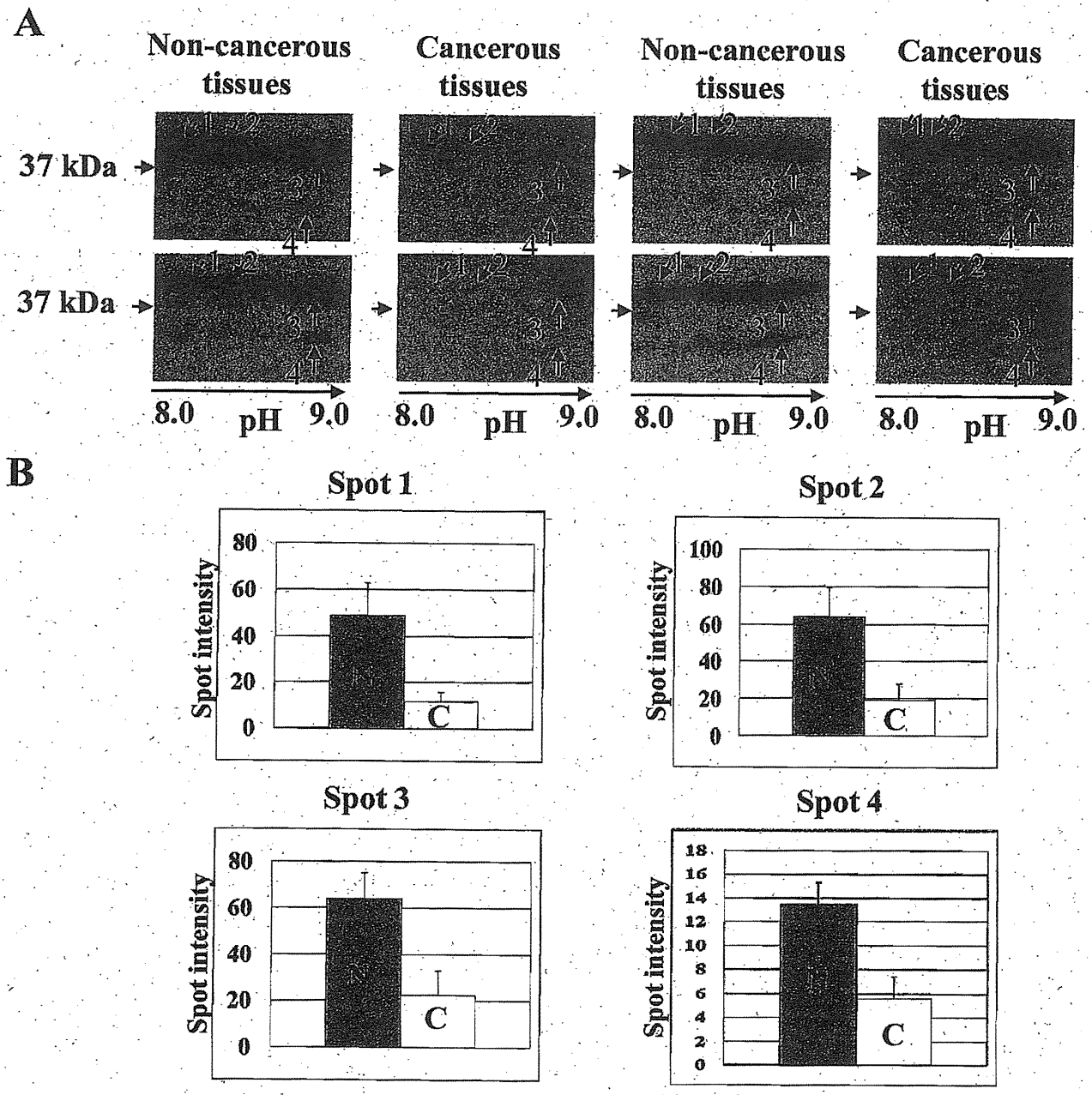

Figure 3. *2-D Western blot analysis of aldolase B. A: Four pairs of cancerous and paired non-cancerous tissues from patients with HCV-HCC underwent 2-D Western blot analysis. Using specific anti-aldolase B antibody, the spots were confirmed as four aldolase B isoforms. Each spot number is the same as those shown in Figure 1A. B: The differential intensities of protein spots in non-cancerous tissues (N) and cancerous tissues (C) in HCC were quantified by Student's t-test (n=4, p<0.05 for each spot). The error bars represent standard errors of the means.*

References

1 El-Serag HB and Mason AC: Rising incidence of hepatocellular carcinoma in the United States. N Engl J Med *340*: 745-750, 1999.

2 Okuda K: Hepatocellular carcinoma. J Hepatol *32*: 225-237, 2000.

3 Yano K, Yatsuhashi H and Yano M: Hepatitis C. Nippon Rinsho *61*: 241-244, 2003 (in Japanese).

4 Castello G, Scala S, Palmieri G, Curley SA and Izzo F: HCV-related hepatocellular carcinoma: From chronic inflammation to cancer. Clin Immunol *134*: 237-250, 2010.

5 Takashima M, Kuramitsu Y, Yokoyama Y, Iizuka N, Toda T, Sakaida I, Okita K, Oka M and Nakamura K: Proteomic

profiling of heat-shock protein 70 family members as biomarkers for hepatitis C virus-related hepatocellular carcinoma. Proteomics *3*: 2487-2493, 2003.

6 Yokoyama Y, Kuramitsu Y, Takashima M, Iizuka N, Toda T, Terai S, Sakaida I, Oka M, Nakamura K and Okita K: Proteomic profiling of proteins decreased in hepatocellular carcinoma from patients infected with hepatitis C virus. Proteomics *4*: 2111-2116, 2004.

7 Kuramitsu Y and Nakamura K: Current progress in proteomic study of hepatitis C virus-related human hepatocellular carcinoma. Expert Rev Proteomics *2*: 589-601, 2005.

8 Mori-Iwamoto S, Kuramitsu Y, Ryozawa S, Mikuria K, Fujimoto M, Maehara S, Maehara Y, Okita K, Nakamura K and Sakaida I: Proteomics finding heat-shock protein 27 as a biomarker for resistance of pancreatic cancer cells to gemcitabine. Int J Oncol *31*: 1345-1350, 2007.

9 Kuramitsu Y, Baron B, Yoshino S, Zhang X, Tanaka T, Yashiro M, Hirakawa K, Oka M and Nakamura K: Proteomic differential display analysis shows up-regulation of 14-3-3 sigma protein in human scirrhous-type gastric carcinoma cells. Anticancer Res *30*: 4459-4465, 2010.

10 Kuramitsu Y, Taba K, Ryozawa S, Yoshida K, Zhang X, Tanaka T, Maehara S, Maehara Y, Sakaida I and Nakamura K: Identification of up- and down-regulated proteins in gemcitabine-resistant pancreatic cancer cells using two-dimensional gel electrophoresis and mass spectrometry. Anticancer Res *30*: 3367-3372, 2010.

11 Kuramitsu Y, Hayashi E, Okada F, Zhang X, Tanaka T, Ueyama Y and Nakamura K: Staining with highly sensitive Coomassie brilliant blue SeePico™ Stain after Flamingo™ fluorescent gel stain is useful for cancer proteomic analysis by means of two-dimensional gel electrophoresis. Anticancer Res *30*: 4001-4005, 2010.

12 Kuramitsu Y, Miyamoto H, Tanaka T, Zhang X, Fujimoto M, Ueda K, Tanaka T, Hamano K and Nakamura K: Proteomic differential display analysis identified up-regulated astrocytic phosphoprotein PEA-15 in human malignant pleural mesothelioma cell lines. Proteomics *9*: 5078-5089, 2009.

13 Takashima M, Kuramitsu Y, Yokoyama Y, Iizuka N, Fujimoto M, Nishisaka T, Okita K, Oka M and Nakamura K: Overexpression of alpha enolase in hepatitis C virus-related hepatocellular carcinoma: association with tumor progression as determined by proteomic analysis. Proteomics *5*: 1686-1692, 2005.

14 Takashima M, Kuramitsu Y, Yokoyama Y, Iizuka N, Harada T, Fujimoto M, Sakaida I, Okita K, Oka M and Nakamura K: Proteomic analysis of autoantibodies in patients with hepatocellular carcinoma. Proteomics *6*: 3894-3900, 2006.

15 Lebherz HG, and Rutter WJ: Distribution of fructose diphosphate aldolase variants in biological systems. Biochemistry *8*: 109-121, 1969.

16 Hers HG and Kusaka T: The metabolism of fructose-1-phosphate in the liver. Biochim Biophys Acta *11*: 427-437, 1953.

17 Rutter WJ, Blostein RE, Woodfin BM and Weber CS: Enzyme variants and metabolic diversification. Adv Enzyme Regul *1*: 39-56, 1963.

18 Kinoshita M and Miyata M: Underexpression of mRNA in human hepatocellular carcinoma focusing on eight loci. Hepatology *36*: 433-438, 2002.

19 Kimura T: Immunoreactivities and messenger RNA expression of aldolase A and B in human hepatoma cell lines. Hokkaido Igaku Zasshi *69*: 1232-1243, 1994 (in Japanese).

20 Castaldo G, Calcagno G, Sibillo R, Cuomo R, Nardone G, Castellano L, Del Vecchio Blanco C, Budillon G and Salvatore F: Quantitative analysis of aldolase A mRNA in liver discriminates between hepatocellular carcinoma and cirrhosis. Clin Chem *46*: 901-906, 2000.

21 Shaw RJ: Glucose metabolism and cancer. Curr Opin Cell Biol *18*: 598-608, 2006.

22 Hamaguchi T, Iizuka N, Tsunedomi R, Hamamoto Y, Miyamoto T, Iida M, Tokuhisa Y, Sakamoto K, Takashima M, Tamesa T and Oka M: Glycolysis module activated by hypoxia-inducible factor 1alpha is related to the aggressive phenotype of hepatocellular carcinoma. Int J Oncol *33*: 725-731, 2008.

23 Rottmann WH, Tolan DR and Penhoet EE: Complete amino acid sequence for human aldolase B derived from cDNA and genomic clones. Proc Natl Acad Sci USA *81*: 2738-2742, 1984.

24 Choi KH, Shi J, Hopkins CE, Tolan DR and Allen KN: Snapshots of catalysis: the structure of fructose-1,6-(*bis*)phosphate aldolase covalently bound to the substrate dihydroxyacetone phosphate. Biochemistry *40*: 13868-13875, 2001.

25 Choi KH, Mazurkie AS, Morris AJ, Utheza D, Tolan DR and Allen KN: Structure of a fructose-1,6-*bis*(phosphate) aldolase liganded to its natural substrate in a cleavage-defective mutant at 2.3 Å. Biochemistry *38*: 12655-12664, 1999.

26 Allen KN: Reaction of enzyme-derived enamines. *In*: Comprehensive Biological Catalysis. Sinnott M (ed.). New York, Academic Press., pp. 135-172, 1998.

27 Arakaki TL, Pezza JA, Cronin MA, Hopkins CE, Zimmer DB, Tolan DR and Allen KN: Structure of human brain fructose 1,6-(*bis*)phosphate aldolase: linking isozyme structure with function. Protein Sci *13*: 3077-3084, 2004.

28 Blom N and Sygusch J: Product binding and role of the *C*-terminal region in class I D-fructose 1,6-*bis*phosphate aldolase. Nat Struct Biol *4*: 36-39, 1997.

29 Wang J, Morris AJ, Tolan DR and Pagliaro L: The molecular nature of the F-actin binding activity of aldolase revealed with site-directed mutants. J Biol Chem *271*: 6861-6865, 1996.

30 Jewett TJ and Sibley LD: Aldolase forms a bridge between cell surface adhesins and the actin cytoskeleton in apicomplexan parasites. Mol Cell *11*: 885-894, 2003.

31 Kiri A and Goldspink G: RNA–protein interactions of the 3' untranslated regions of myosin heavy chain transcripts. J Muscle Res Cell Motil *23*: 119-129, 2002.

32 Karkhoff-Schweizer R and Knull HR: Demonstration of tubulin-glycolytic enzyme interactions using a novel electrophoretic approach. Biochem Biophys Res Commun *146*: 827-831, 1987.

33 Kusakabe T, Motoki K and Hori K: Mode of interactions of human aldolase isozymes with cytoskeletons. Arch Biochem Biophys *344*: 184-193, 1997.

Received June 8, 2011
Revised July 13, 2011
Accepted July 14, 2011

ANTICANCER RESEARCH *31*: 3331-3336 (2011)

Up-regulation of 42 kDa Tubulin Alpha-6 Chain Fragment in Well-differentiated Hepatocellular Carcinoma Tissues from Patients Infected with Hepatitis C Virus

YASUHIRO KURAMITSU[1], MOTONARI TAKASHIMA[1,2], YUICHIRO YOKOYAMA[1,3], NORIO IIZUKA[2], TAKAO TAMESA[2], JUNKO K. AKADA[1], YUFENG WANG[1], TOSHIFUSA TODA[4], ISAO SAKAIDA[3], KIWAMU OKITA[3], MASAAKI OKA[2] and KAZUYUKI NAKAMURA[1]

Departments of [1]Biochemistry and Functional Proteomics, [2]Surgery and Clinical Science; and [3]Hepatology and Gastroenterology, Yamaguchi University Graduate School of Medicine, Ube, Japan; [4]Tokyo Metropolitan Institute of Gerontology, Tokyo, Japan

Abstract. *We performed proteomic differential display analysis of hepatitis C virus-associated 21 human hepatocellular carcinoma (HCV-HCC) tissues by using two-dimensional gel electrophoresis (2-DE) and matrix-assisted laser desorption/ionization time-of-flight mass spectrometry (MALDI-TOF/MS). One of the numerous spots which was located next to three spots of glutamine synthetase showed stronger intensity in well-differentiated HCC tissues compared to non-cancerous tissues. Samples from 6 out of 21 patients showed up-regulation of this spot compared to non-cancerous tissues. After in-gel digestion, MALDI-TOF/MS identified the spot as tubulin alpha-6 chain. Two-dimensional immunoblot analysis confirmed that this spot was indeed tubulin alpha, and this spot was stronger in cancerous tissues than in noncancerous tissues. These results suggest that tubulin alpha-6 chain is one of the candidates for biomarkers for well-differentiated HCV-associated HCC.*

Hepatocellular carcinoma (HCC) is one of the most common types of cancer worldwide, with a high incidence in many countries. Although the causes of HCC are recognized as infection with hepatitis virus, exposure to aflatoxin B1 and alcoholic drinking habit, infection with hepatitis C virus (HCV) is the most clearly established risk factor for HCC in developed countries, including Japan. On the other hand, in developing countries, infection with hepatitis B virus (HBV) is the clearest risk factor for HCC. HCC cells progress through a multistep process based on histological changes. Although initially HCC tumour cells are well-differentiated, they dedifferentiate to become moderately or poorly differentiated, with high proliferation rates with the progression of the tumour. Therefore, it is very important to diagnose HCC at the stage of the well-differentiated form (1-4).

In recent studies, we have reported proteomic analysis for HCV-associated HCC tissues by the combination of two-dimensional gel electrophoresis (2-DE) and mass spectrometry (MS), which is a proteomic method of high-throughput analysis of protein expression. These studies have identified diverse proteins that may be involved in the pathogenic mechanism of HCC (5-8). In these proteomic studies, we identified alpha enolase as being up-regulated in poorly differentiated HCV-associated HCC tissues (9), and glutamine synthetase isoforms as being up-regulated in well-differentiated HCV-associated HCC tissues (10). Both are expected to be biomarkers for poorly and well-differentiated HCV-associated HCC.

In the present study, we performed proteomic analysis for 21 pairs of HCV-associated HCC tissues and corresponding non-cancerous tissues to find proteins that might be involved in tumour differentiation and progression. Since in well-differentiated HCV-associated HCC tissues a spot of approximately 42 kDa in MW with a *p*I of 7.0 showed stronger intensity compared with that in non-cancerous samples, we further analyzed this spot.

Materials and Methods

Tissue samples. Twenty-one pairs of cancerous tissues and adjacent non-cancerous liver tissues were obtained from patients who had been diagnosed as having HCV-associated HCC and had undergone surgical liver resection at the Yamaguchi University School of Medicine from May 1997 to December 2000. The histological diagnosis of HCC was made from the formalin-fixed, paraffin-embedded tissues after surgery

Correspondence to: Yasuhiro Kuramitsu, MD, Ph.D., Department of Biochemistry and Functional Proteomics, Yamaguchi University Graduate School of Medicine, 1-1-1 Minami-Kogushi, Ube, Yamaguchi 755-8505, Japan. Tel: +81 836222213, Fax: +81 836222212, e-mail: climates@yamaguchi-u.ac.jp

Key Words: Tubulin alpha-6 chain, HCV-HCC, proteomics, 2-DE, MS.

according to the World Health Organization criteria (Pathology and Genetics. Tumours of the Digestive System. WHO Classification of Tumours, Volume 2, Third Edition, 2000) in all cases. None was positive for hepatitis B surface antigen. Informed consent in writing had been obtained from all patients before surgery. The study protocol was approved by the Institutional Review Board for Human Use of the Yamaguchi University School of Medicine.

Sample preparation. The liver tissues were suspended and homogenized in lysis buffer (50 mM Tris-HCl, pH 7.5, 165 mM NaCl, 10 mM NaF, 1 mM sodium vanadate, 1 mM phenylmethylsulfonyl fluoride (PMSF), 10 mM EDTA, 10 μg/ml aprotinin, 10 μg/ml leupeptin, and 1% NP40). After centrifugation at 15,000 ×*g* for 30 min at 4˚C, the supernatants were taken and used as samples (6-10).

Two-dimensional gel electrophoresis (2-DE). Three hundred micrograms of protein was used for each electrophoresis. The first dimensional isoelectric focusing (IEF) was performed in an IPGphor3 IEF unit (GE Healthcare, Buckinghamshire, UK) on 7 cm, immobilized, pH 3-10 linear gradient strips (Bio-Rad, Hercules, CA, USA) at 50 μA/strip. The strips were rehydrated with 125 μl sample containing 8 M urea, 2% CHAPS, 0.01% bromophenol blue, dithiothreitol (DTT), and immobilized pH gradient (IPG) buffer, for 14 h. IEF was then run in 3 steps, at 500 V for 1 h, 1000 V for 1 h, and 8000 V for 2 h. The second dimension was performed on SDS-polyacrylamide gels. After electrophoresis, the gels were stained with Coomassie Brilliant Blue (CBB) R250 (Nacalai Tesque, Kyoto, Japan) for 24 h. They were destained with 10% acetic acid in water containing methanol for 30 min, and again destained with 7% acetic acid (6-10).

Image analysis. The positions of the protein spots on the gels obtained using samples of non-cancerous and cancerous tissues were recorded with an Agfa ARCUS 1200 image scanner (Agfa-Gevaert N.V., Mortsel, Belgium) and were analyzed with Image Master 2D Platinum ver. 5.0 (GE Healthcare). Spots present at different intensities were excised from the gels for MS analysis (6-10).

In-gel digestion. The CBB dye was removed by rinsing twice in 60% methanol, containing 50 mM ammonium bicarbonate and 5 mM DTT, for 15 min, and twice in 50% acetonitrile, containing 50 mM ammonium bicarbonate and 5 mM DTT, for 7 min. The gel piece was dehydrated in 100% acetonitrile, and then re-swollen with an in-gel digestion reagent containing 10 μg/ml sequencing grade trypsin (Promega V5111, Madison, WI, USA) in 30% acetonitrile, containing 50 mM ammonium bicarbonate and 5 mM DTT. In-gel digestion was carried out overnight at 30˚C (6-10).

Peptide mass fingerprinting (PMF). After the in-gel digestion, 1 μl of the reaction mixture was removed and mixed with 1 μl of the matrix solution (10 mg/ml alpha-cyano-4-hydroxycinnamic acid in 50% acetonitrile, 40% methanol, 0.1% trifluoroacetic acid (TFA)) on a MALDI target plate. The MALDI-TOF/MS for PMF was performed on a Shimadzu Biotech AXIMA-CFR mass spectrometer in a reflectron mode. The MS-Fit database search engine at the ProteinProspecter web site (http://prospeoter.ucsf.edu/) was used for the protein identification (6, 7).

Two-dimensional immunoblot analysis. After 2-DE, fractionated proteins (50 μg) were transferred electrophoretically onto poly-vinylidene difluoride (PVDF) membranes (Immobilon-P; Millipore Corporation, Bedford, MA, USA), and the membranes were blocked overnight at 4˚C in Tris-buffered saline (TBS) containing 5% skim milk. The primary antibody was a mouse anti-alpha tubulin monoclonal antibody (1:4000; Sigma-Aldrich, St. Louis, MO, USA). The membranes were then incubated for 1 h at 4˚C, washed four times with TBS containing 0.05% Tween 20, and incubated for 1 h at 4˚C with horseradish peroxidase-conjugated secondary antibody (1:5000; Jackson ImmunoResearch Laboratories Inc, West Grove, PA, USA). The reaction was visualized with a chemiluminescence reagent (ImmunoStar Long Detection, Wako, Osaka, Japan) and scanned by using Image Reader LAS-1000 Pro (Fujifilm Corporation, Tokyo, Japan) (10, 11).

Results

Identification of proteins on 2-DE gels. We have already reported proteomic analysis of cancerous and non-cancerous tissues of HCV-associated HCC, and showed that there were three spots of glutamine synthetase (GS) showing stronger intensity in the cancerous tissues of well-differentiated HCC than in the non-cancerous tissues (10). Besides these three spots (spots 1-3 in Figure 1B), a spot of approximately 42 kDa in MW with a *p*I of 7.0 (spot 4) showed stronger intensity in well-differentiated HCC tissues than in non-cancerous samples (Figure 1A). While the up-regulation of this spot was seen in 6/21 samples, in the samples of well-differentiated HCC tissues, up-regulation was found in 3/4. The spot was digested and analyzed by MS. This sample provided a good spectrum of amino acid sequences by MALDI-TOF/MS and the protein was identified as tubulin alpha-6 chain. Peptide sequences of tubulin alpha-6 chain were identified as (K)EIIDLVLDR(I), (K)YMACCLLYR(G), (R)LDHKFDLMYAK(R), (R)TIQFV DWCPTGFK(V), (R)AVFVDLEPTVIDEVR(T) and (R)NLDI ERPTYTNLNR(L) by MS spectra of trypsin-digested sample. The expression of this protein was confirmed by 2-D immunoblot analysis. The position of this spot was confirmed and the intensity of this spot was stronger in cancerous tissues than in noncancerous tissues (Figure 2).

Discussion

Up-regulation of tubulin alpha-6 chain in the well-differentiated HCV-associated HCC tissues was observed on the 2-DE gels, and immunoblot analysis with specific anti-alpha tubulin mAb confirmed that this spot was tubulin alpha-6 chain.

Tubulin forms microtubules by means of the polymerization of tubulin alpha and beta heterodimers. This assembly and disassembly of tubulin into microtubules is assisted by other factors such as the binding of microtubule-associated proteins. This dynamic state is characterized by growth randomly interrupted by pauses and shrinkage. Microtubules play critical roles in diverse cellular functions. They are essential components of all cells, and play roles as essential factors in intracellular signaling, cellular morphology and mitosis (12). Since microtubules play important roles in mitosis, microtubule-destabilizing agents and -stabilizing agents have been used for anticancer therapy.

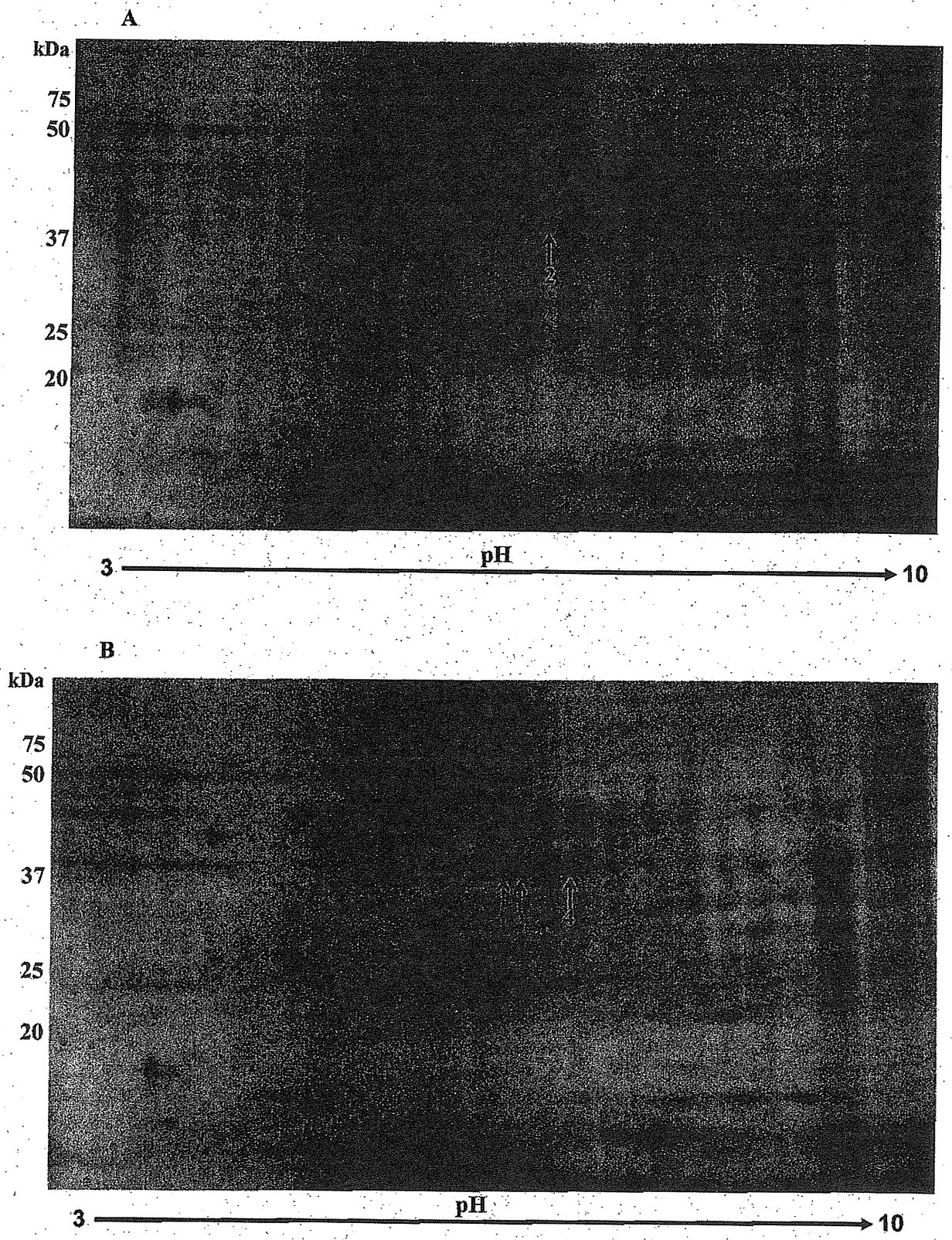

Figure 1. *2-DE patterns of spots for four proteins in tissues from patients with hepatocellular carcinoma infected with HCV. Protein samples (300 μg) were loaded onto the gel. A: Non-cancerous and B: cancerous tissues. Arrows indicate four strongly stained protein spots of 42 kDa and with pI 6.4-7.0. Spots 1-3 have been already reported as liver glutamine synthetase, including phosphorylated forms.*

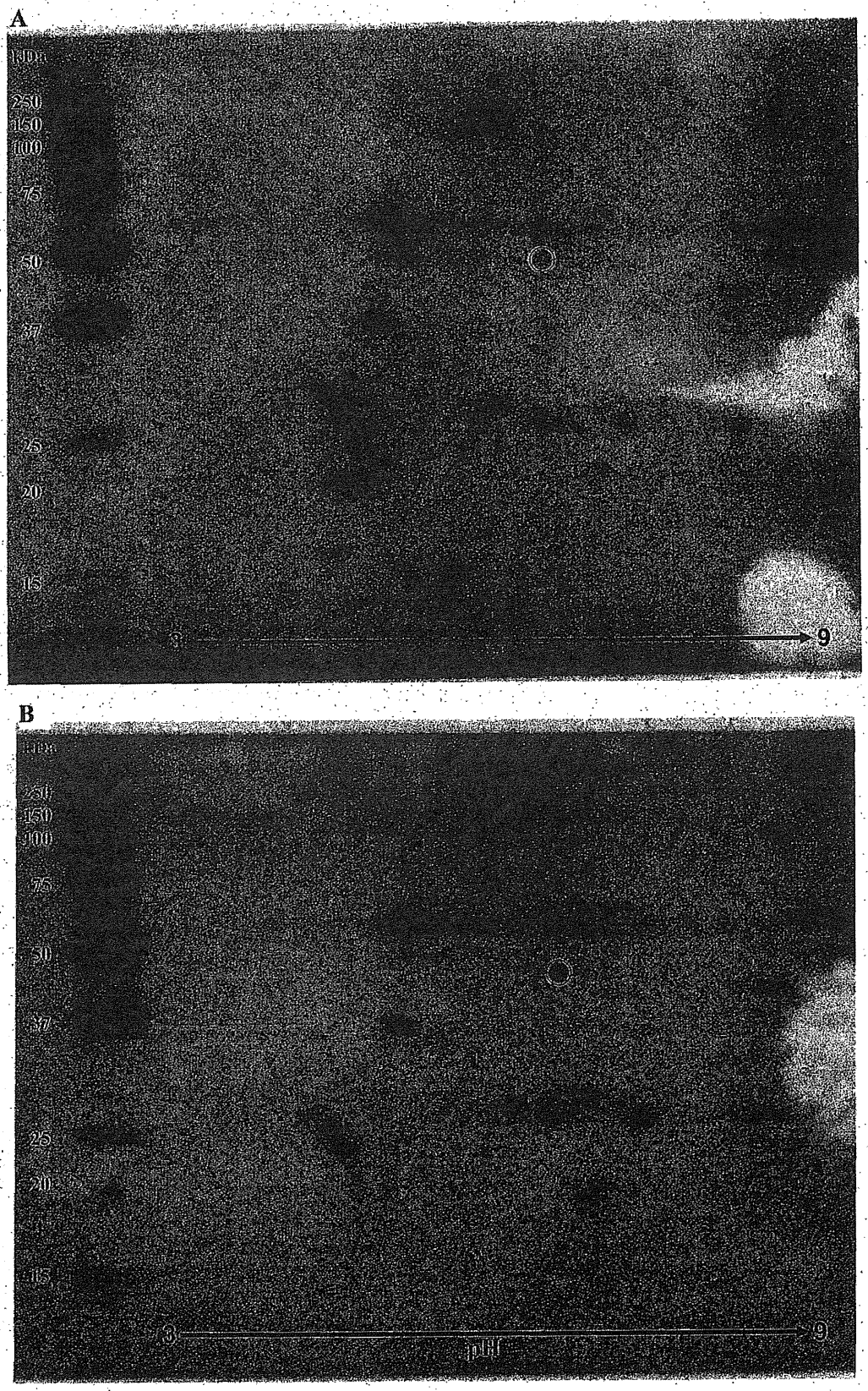

Figure 2. *Continued*

3334

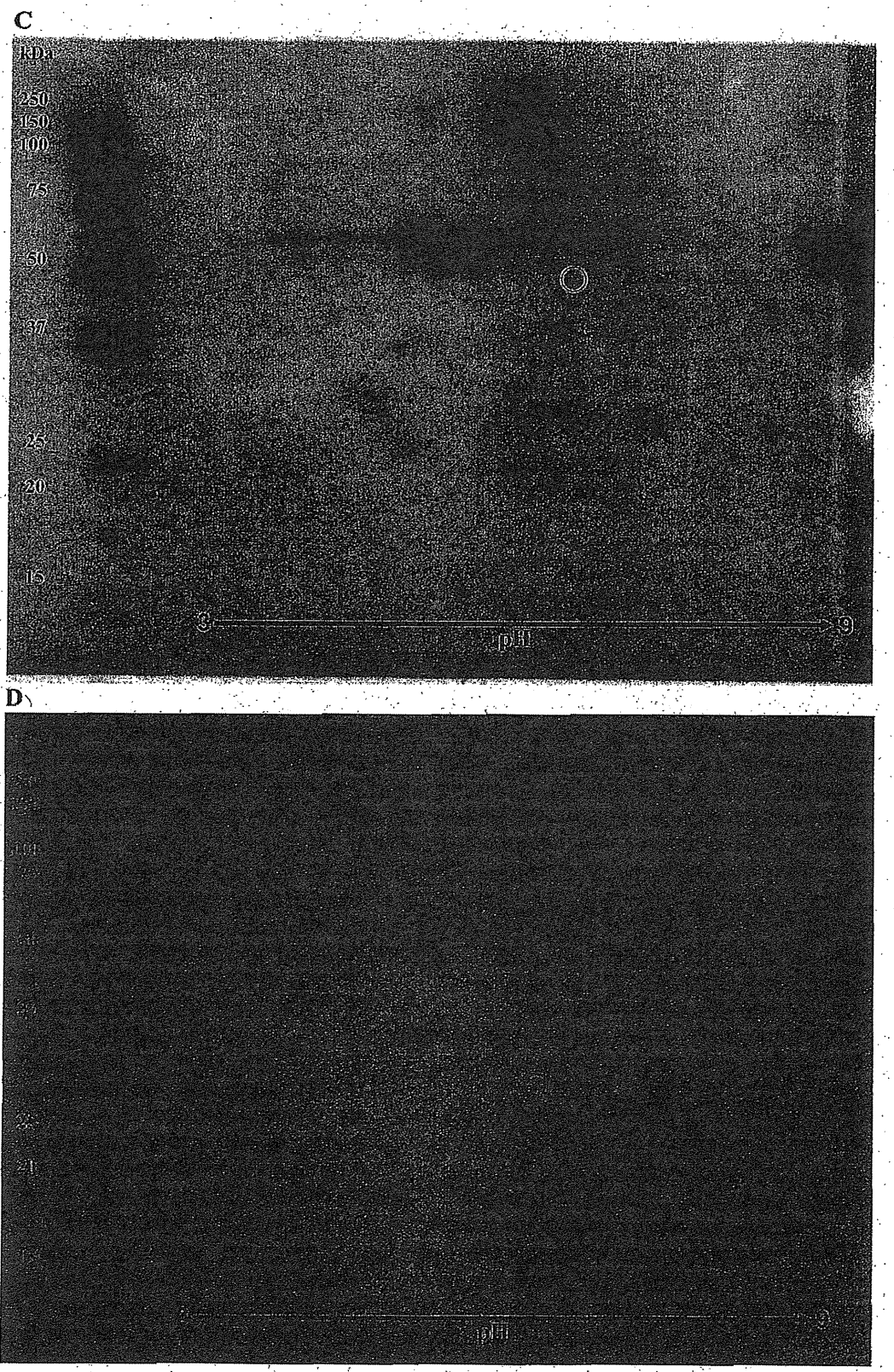

Figure 2. *2-D immunoblot analysis of alpha-tubulin in non-cancerous and paired cancerous tissues. For the 2-D immunoblot analysis, 50 μg protein of non-cancerous (A, C) and cancerous (B, D) tissues was applied. Expression of alpha-tubulin was confirmed; the intensity of the spot was stronger in cancerous tissue than non-cancerous tissue. The spot (40 kDa, pI 7.0) marked by a circle was confirmed as being alpha-tubulin.*

Microtubule-destabilizing agents, such as vinblastine and vincristine, inhibit polymerization of microtubules, resulting in the inhibition of mitosis; microtubule-destabilizing agents, such as taxanes, stabilize polymerized microtubules, arresting mitosis and apoptosis (13, 14).

Overexpression of tubulins in tumour tissues have been reported by many groups. Matos *et al.* reported beta-5-tubulin was up-regulated in HCC in the USA (15). He *et al.* showed tubulin beta-2C to be up-regulated in sentinel lymph nodes of colorectal cancer (16). Not only beta-tubulins, but also overexpression of alpha-tubulins in tumour tissues have been reported by many groups. In tissues of pulmonary sclerosing haemangioma, small cell lung cancer, renal cell carcinoma and oesophageal squamous cell carcinoma, overexpression of tubulin alpha proteins has been detected (17-20). Furthermore, overexpression of tubulin alpha 6 chain has been also reported in gastric cancer and ovarian cancer (21, 22). However, no report has shown increased fragment of alpha-tubulin in tumour tissues. The molecular weight of the up-regulated tubulin alpha-6 chain fragment in HCV-associated HCC tissues here was 42 kDa. Tubulin alpha-6 chain reported by Wu *et al.* (21) and Lim *et al.* (22) was of about 50 kDa. This would apparently seem to be different from our reported tubulin alpha-6 chain fragment. As yet, no report about digesting enzyme for tubulin alpha-6 chain has been published. Therefore, it is important to clarify the mechanism of overexpression of 42 kDa tubulin alpha-6 chain fragment in well-differentiated HCV-associated HCC tissues.

References

1 El-Serag HB and Mason AC: Rising incidence of hepatocellular carcinoma in the United States. N Eng J Med *340*: 745-750, 1999.
2 Tanaka E and Kiyosawa K: Natural history of acute hepatitis C. Gastroenterol Hepatol *15*: E97-E104, 2000.
3 Niederau C, Lange S, Heintges T, Erhardt A, Buschkamp M, Hürter D, Nawrocki M, Kruska L, Hensel F, Petry W and Häussinger D: Prognosis of chronic hepatitis C: results of a large, prospective cohort study. Hepatology *28*: 1687-1695, 2003.
4 Okuda K: Hepatocellular carcinoma. J Hepatol *32*: 225-237, 2000.
5 Kuramitsu Y and Nakamura K: Current progress in proteomic study of hepatitis C virus-related human hepatocellular carcinoma. Expert Rev Proteomics *2*: 589-601, 2005.
6 Takashima M, Kuramitsu Y, Yokoyama Y, Iizuka N, Toda T, Saiakida I, Okita K, Oka M and Nakamura K: Proteomic profiling of heat-shock protein 70 family members as biomarkers for hepatitis C virus-related hepatocellular carcinoma. Proteomics *3*: 2487-2493, 2003.
7 Yokoyama Y, Kuramitsu Y, Takashima M, Iizuka N, Toda T, Terai S, Sakaida I, Oka M, Nakamura K and Okita K: Proteomic profiling of proteins decreased in hepatocellular carcinoma from patients infected with hepatitis C virus. Proteomics *4*: 2111-2116, 2004.
8 Takashima M, Kuramitsu Y, Yokoyama Y, Iizuka N, Fujimoto M, Sakaida I, Okita K, Oka M and Nakamura K: Proteomic analysis of autoantibodies in patients with hepatocellular carcinoma. Proteomics *6*: 3894-3900, 2006.
9 Takashima M, Kuramitsu Y, Yokoyama Y, Iizuka N, Fujimoto M, Nishisaka T, Sakaida I, Okita K, Oka M and Nakamura K: Overexpression of alpha enolase in hepatitis C virus-related hepatocellular carcinoma: association with tumor progression as determined by proteomic analysis. Proteomics *5*: 1686-1692, 2005.
10 Kuramitsu Y, Harada T, Takashima M, Yokoyama Y, Hidaka I, Iizuka N, Toda T, Fujimoto M, Zhang X, Sakaida I, Okita K, Oka M and Nakamura K: Increased expression, and phosphorylation of liver glutamine synthetase in well-differentiated hepatocellular carcinoma tissues of patients infected with hepatitis C virus. Electrophoresis *27*: 1651-1658, 2006.
11 Tanaka T, Kuramitsu Y, Fujimoto M, Naito S, Oka M and Nakamura K: Down-regulation of two isoforms of ubiquitin carboxyl-terminal hydrolase isozyme L1 (UCH-L1) correlates with high metastatic potentials of human SN12C renal cell carcinoma cell clones. Electrophoresis *29*: 2651-2659, 2008.
12 Wade RH: On and around microtubules: an overview. Mol Biotechnol *43*: 177-191, 2009.
13 Yue QX, Liu X and Guo DA: Microtubule-binding natural products for cancer therapy. Planta Med *76*: 1037-1043, 2010.
14 Perez EA: Microtubule inhibitors: Differentiating tubulin-inhibiting agents based on mechanisms of action, clinical activity, and resistance. Mol Cancer Ther *8*: 2086-2095, 2009.
15 Matos JM, Witzmann FA, Cummings OW and Schmidt CM: A pilot study of proteomic profiles of human hepatocellular carcinoma in the United States. J Surg Res *155*: 237-243, 2008.
16 He ZY, Wen H, Shi CB and Wang J: Up-regulation of hnRNP A1, ezrin, tubulin β-2C and annexin A1 in sentinel lymph nodes of colorectal cancer. World J Gastroenterol *16*: 4670-4676, 2010.
17 Cho SJ, Jin LJ, Kim BY, Cho SI, Jung WY, Han JH, Ha SY, Kim HK and Kim A: Increased expression of matrix metalloproteinase 9 and tubulin-alpha in pulmonary sclerosing hemangioma. Oncol Rep *18*: 1139-1144, 2007.
18 Jeong HC, Kim GI, Cho SH, Lee KH, Ko JJ, Yang JH and Chung KH: Proteomic analysis of human small cell lung cancer tissues: up-regulation of coactosin-like protein-1. J Proteome Res *10*: 269-276, 2011.
19 Seliger B, Dressler SP, Wang E, Kellner R, Recktenwald CV, Lottspeich F, Marincola FM, Baumgärtner M, Atkins D and Lichtenfels R: Combined analysis of transcriptome and proteome data as a tool for the identification of candidate biomarkers in renal cell carcinoma. Proteomics *9*: 1567-1581, 2009.
20 Qi Y, Chiu JF, Wang L, Kwong DL and He QY: Comparative proteomic analysis of esophageal squamous cell carcinoma. Proteomics *5*: 2960-2971, 2005.
21 Wu C, Luo Z, Chen X, Wu C, Yao D, Zhao P, Liu L, Shi B and Zhu L: Two-dimensional differential in-gel electrophoresis for identification of gastric cancer-specific protein markers. Oncol Rep *21*: 1429-1437, 2009.
22 Lim R, Lappas M, Ahmed N, Permezel M, Quinn MA and Rice GE: 2D-PAGE of ovarian cancer: analysis of soluble and insoluble fractions using medium-range immobilized pH gradients. Biochem Biophys Res Commun *406*: 408-413, 2011.

Received June 15, 2011
Revised July 21, 2011
Accepted July 22, 2011

Differential expression of up-regulated cofilin-1 and down-regulated cofilin-2 characteristic of pancreatic cancer tissues

YUFENG WANG[1], YASUHIRO KURAMITSU[1], TOMIO UENO[2], NOBUAKI SUZUKI[2], SHIGEFUMI YOSHINO[2], NORIO IIZUKA[2], XIULIAN ZHANG[1], MASAAKI OKA[2] and KAZUYUKI NAKAMURA[1]

Departments of [1]Biochemistry and Functional Proteomics and [2]Digestive Surgery of Applied Molecular Bioscience, Yamaguchi University Graduate School of Medicine, Ube, Yamaguchi 755-8505, Japan

Received June 29, 2011; Accepted July 28, 2011

DOI: 10.3892/or.2011.1447

Abstract. Pancreatic cancer (PC) is one of the most deadly malignant tumors. The aim of this study was to identify potential biomarkers for PC. Using two-dimensional gel electrophoresis and liquid chromatography-tandem mass spectrometry, the proteomic profiles of pancreatic cancerous and non-cancerous tissues from ten patients with PC were compared. One of the numerous spots that showed stronger intensity in cancerous compared to non-cancerous tissues was identified as non-muscle cofilin (cofilin-1). This up-regulation was validated by Western blot analysis. It is noteworthy that Western blot analysis showed significantly lower expression of muscle cofilin (cofilin-2) in pancreatic cancerous tissues compared to non-cancerous tissues. This is the first time that cofilin isoforms (cofilin-1/2) have been identified to be differentially expressed in pancreatic cancerous tissues. Therefore, cofilin isoforms may serve as candidates for clinically useful biomarkers or therapeutic targets for PC.

Introduction

Pancreatic cancer (PC) is a malignant tumor which is associated with an extremely unfavorable prognosis. Because of delayed diagnosis and the lack of response to various therapies, few patients with PC survive for more than 5 years; due to rapid aggressiveness, most cases are diagnosed after metastatic spread (1). Therefore, it is critical to discover more sensitive biomarkers for the diagnosis of patients with PC, and the biological mechanisms involved in the extreme aggressiveness of PC should be clarified.

Correspondence to: Dr Yasuhiro Kuramitsu, Department of Biochemistry and Functional Proteomics, Yamaguchi University Graduate School of Medicine, 1-1-1 Minami-Kogushi, Ube, Yamaguchi 755-8505, Japan
E-mail: climates@yamaguchi-u.ac.jp

Key words: two-dimensional gel electrophoresis, liquid chromatography-tandem mass spectrometry, pancreatic cancer, cofilin-1/2

Proteomics has been widely applied to discover candidate biomarkers in various types of cancers. Using proteomic differential display analysis, research groups have identified biomarkers such as PEA-15 in human malignant pleural mesothelioma cell lines, heat-shock proteins (Hsp27, Hsp70, GRP78) in hepatocellular carcinoma, numerous candidate proteins in colorectal cancer and α-1-antitrypsin isoforms as a possible serum biomarker in pancreatic cancer (2-6). Proteomic technology that combines two-dimensional gel electrophoresis (2-DE) and liquid chromatography-tandem mass spectrometry (LC-MS/MS) has high throughput and accuracy, and these technologies are considered as useful tools to comprehensively analyze proteins.

Using these techniques, we found that cofilin-1 displayed differential expression on 2-DE gels between pancreatic cancerous and non-cancerous tissue samples. Western blotting demonstrated that cofilin-1 was significantly up-regulated in cancerous tissues compare to non-cancerous tissues; but opposingly cofilin-2 expression was significantly diminished in cancerous tissues. The findings of the present study incite an interest in cofilin and focus on the relationship between cofilin isoforms and cancer progression.

Materials and methods

Sample preparation. Twenty-four pairs of pancreatic non-cancerous and cancerous tissues were collected from 24 patients diagnosed with PC who underwent surgical resection of the pancreas at the Department of Surgery II, Yamaguchi University Hospital. None of the patients received any pre-operative therapy. Written informed consent was obtained from all patients before surgery. The study protocol was approved by the Institutional Review Board for Human Research of the Yamaguchi University School of Medicine.

Tissues were homogenized in lysis buffer (1% NP-40, 1 mM sodium vanadate, 1 mM PMSF, 10 mM NaF, 10 mM EDTA, 50 mM Tris, 165 mM NaCl, 10 μg/ml leupeptin and 10 μg/ml aprotinin) on ice (5). After centrifugation (21,500 x g, 30 min, 4°C), the supernatants were used as samples. Ten pairs from the samples were used for 2-DE, and 24 pairs were used for Western blotting.

Two-dimensional electrophoresis. Isoelectric focusing (IEF) was performed in an IPGphor 3 IEF unit (GE Healthcare, Buckinghamshire, UK) on 11 cm, immobilized linear pH gradient, pH 3.0-10.0 linear gradient IPG strips (Bio-Rad, Hercules, CA, USA) at 50 μA/strip. Samples were mixed with 200 μl of rehydration buffer [8 M urea, 2% CHAPS, 0.01% bromophenol blue, 1.2% Destreak reagent (GE Healthcare, Uppsala, Sweden)] and 0.5% IPG buffer (GE Healthcare) and loaded into the IPGphor strip holder (GE Healthcare). Eighty micrograms of protein was loaded for each 2-DE. The IEF was performed overnight according to the following program: rehydration for 10 h (0 V); 0-500 V for 4 h; 500-1,000 V for 1 h; 1,000-8,000 V for 4 h; 8,000 V for 20 min; and the final phase of 500 V from 20,000-30,000 Vh (7).

The IPG strips were equilibrated in equilibration buffer 1 (6 M urea, 0.5 M Tris-HCl pH 8.8, 30% glycerol, 2% SDS, 2% 2-ME) for 10 min and buffer 2 (6 M urea, 0.5 M Tris-HCl pH 8.8, 30% glycerol, 2% SDS, 2.5% iodoacetoamide) for another 10 min. The IPG strips were then transferred onto the gels, run at 200 V; SDS-PAGE was performed on a precast-polyacrylamide gel with a linear concentration gradient of 5-20% (Bio-Rad) (8,9). Each sample was repeated three times to ensure protein pattern reproducibility.

Fluorescence staining and image analysis. After washing with Milli-Q water 3 times, the SDS-PAGE gels were incubated with 40% ethanol and 10% acetic acid for 2.5 h. After fixation, the gel were then stained with a fluorescent gel staining, Flamingo™ Fluorescent Gel Stain (Bio-Rad) overnight (10). The stained gels were rinsed with Milli-Q water 5 times on a shaker for 5 min. The gels were scanned by using the ProXpress 2-D Proteomic Imaging System (PerkinElmer, Waltham, MA, USA) and then analyzed using Progenesis Samespots software (Nonlinear, Newcastle upon Tyne, UK). Subsequently, the gels were stained with SeePico™ (Benebiosis, Seoul, Korea) overnight (11). The protein spots showing different intensities were picked up from the gels and analyzed with LC-MS/MS.

Liquid chromatography tandem mass spectrometry analysis. The gel pieces were digested with trypsin and lyophilized overnight with the use of Labconco Lyph-lock 1L Model 77400 (Labconco, Kansas City, MO, USA). Lyophilized samples were dissolved in 15 μl of 0.1% formic acid, and then analyzed using the LC-MS/MS system. Peptide sequencing of the identified protein spot was performed using LC-MS/MS with a Spectrum Mill MS Proteomics Workbench (Agilent Technology, Palo Alto, CA, USA).

Western blotting. Samples were separated by electrophoresis with SDS-PAGE gels and then transfered onto PVDF membranes at 90 mA for 78 min. The PVDF membranes were blocked overnight with TBS containing 5% milk at 4°C (12). The membranes were incubated with the primary antibody against cofilin-1 (anti-CFL1 mouse monoclonal antibody, 1:1,000; Sigma, St. Louis, MO, USA) or cofilin-2 (anti-CFL2 goat polyclonal antibody, 1:1,000; Santa Cruz Biotechnology, Inc., Santa Cruz, CA) overnight at 4°C. The membranes were further incubated with the secondary antibody conjugated with horseradish peroxidase (1:10,000) for 1 h at room temperature. The membranes were then reacted with a chemiluminescent reagent (ImmunoStar Long Detection; Wako, Osaka, Japan) and scanned using the Image Reader LAS-1000 Pro (FujiFilm Corporation, Tokyo, Japan).

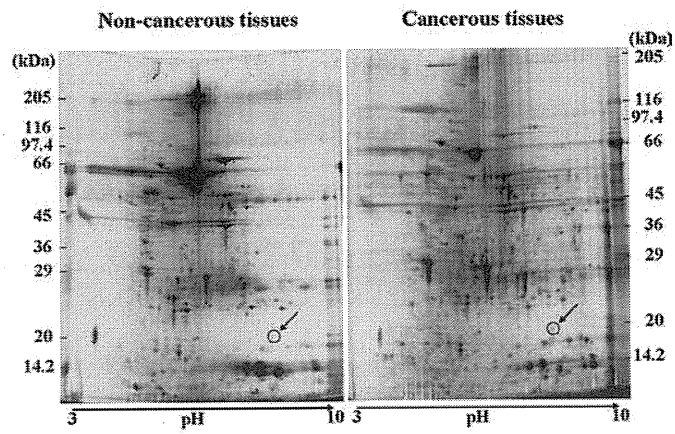

Figure 1. Two-dimensional gel electrophoresis image of pancreatic cancerous and paired non-cancerous tissues stained with Flamingo™ Gel Staining and scanned using the ProXpress 2-D Proteomic Imaging system. Proteins were separated on pH 3.0-10.0 linear, immobilized pH gradient strips and then by 12.5% SDS-PAGE. The spot (indicated by a circle and an arrow) exhibited a stronger intensity on the gel from the cancerous tissue compared to the non-cancerous tissue.

Results

2-DE in the pancreatic non-cancerous and cancerous tissues. 2-DE gels were stained with a fluorescent gel staining and analyzed using Progenesis Samespots software. At least 300 protein spots were matched on each 2-DE gel. A spot of ~20 kDa in mass with an isoelectric point (pI) 8.0 showed stronger intensity in the pancreatic cancerous tissues than in the non-cancerous tissues (Figs. 1 and 2A). The quantification information is summarized in Table I.

Protein identification by LC-MS/MS. Cofilin-1 was identified as the up-regulated protein spot on the 2-DE gels. The peptide sequence of cofilin-1 was identified as (K) LGGSAVISLEGKPL(-) by MS and MS/MS spectra of trypsin-digested gels. MS/MS data for this protein are summarized in Table I.

Western blot analysis of cofilin isoforms (cofilin-1/2). Cofilin-1 on the 2-DE gels was identified by 2-D gel electrophoresis and Western blotting (Fig. 2B). Twenty-four pairs of cancerous and non-cancerous tissues were analyzed by Western blotting using the anti-cofilin-1 (Fig. 3A) or the anti-cofilin-2 antibody (Fig. 4A). The different intensities of the bands between the cancerous and non-cancerous tissues were quantified by the Student's t-test. The expression of cofilin-1 was increased in the pancreatic cancerous tissues when compared to the non-cancerous tissues (22/24; 91.6%), (Fig. 3A). The intensities of the bands of cofilin-1 in the cancerous and non-cancerous tissue samples were 116.3 and 31.7 ($p<0.001$), respectively (Fig. 3B). The intensities of the bands of cofilin-2 in the cancerous and non-cancerous tissues samples were 67.4 and 9.1 ($p<0.001$), respectively (Fig. 4B). The expression of cofilin-2 was

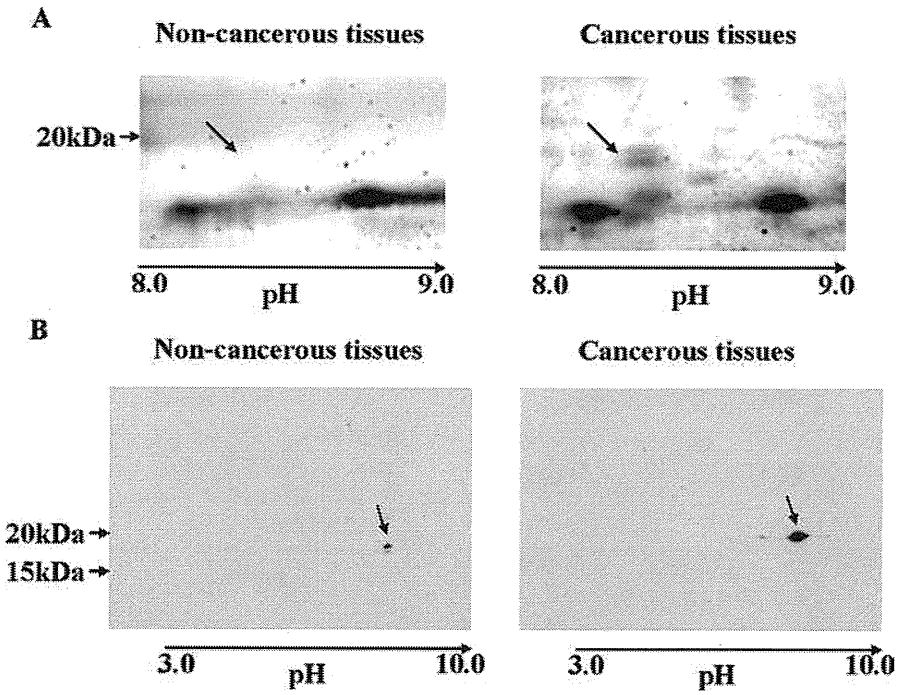

Figure 2. Up-regulated expression of the spot as determined by two-dimensional gel electrophoresis (2-DE) and 2-D Western blotting between cancerous and paired non-cancerous tissues. (A) Differential intensity of the spot between the cancerous tissue compared to the paired non-cancerous tissue as shown on 2-DE gels. (B) Localization of the spot (cofilin-1) was displayed on PDVF membranes by 2-D Western blotting using the anti-cofilin-1 antibody.

Table I. Identification and intensity of the up-regulated protein spot in the cancerous tissues.

Protein	Accession no.	pI/Mr[a]	Peptide[b]	Intensity[c]	Frequency	p-value
Cofilin-1	P23528	8.22/18502.6	(K)LGGSAVISLEGKPL(-)	1.8	8/10	0.005

[a]Theoretical pI and molecular weight (Da) from the protein database. [b]Peptide sequencing of cofilin-1 was identified by LC-MS/MS analysis. [c]Ratio of spot intensity in cancerous to non-cancerous tissues on 2-DE gels.

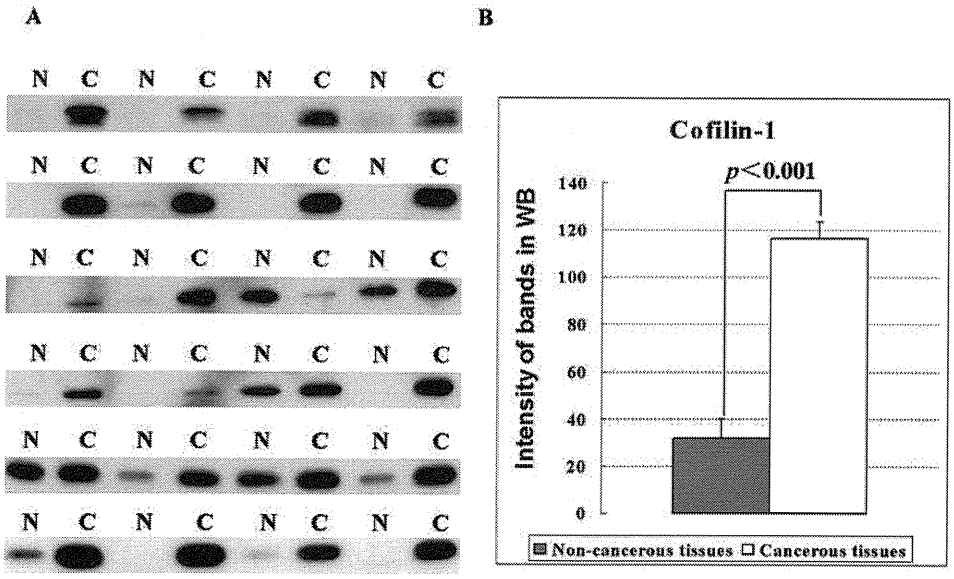

Figure 3. Western blot analysis of cofilin-1 was carried out in pancreatic cancerous and paired non-cancerous tissues. (A) Pancreatic cancerous (C) and paired non-cancerous (N) tissues from 24 PC patients were used, and the anti-cofilin-1 antibody was applied. The expression of cofilin-1 was increased in the pancreatic cancerous tissues compared to that in the paired non-cancerous tissues (91.67%). (B) Comparison of the intensity of the bands between the cancerous and non-cancerous tissues by the Student's t-test (n=24, p<0.001). The relative standard errors (SE) of cancerous and non-cancerous tissue samples were 8.112 and 6.852, respectively.

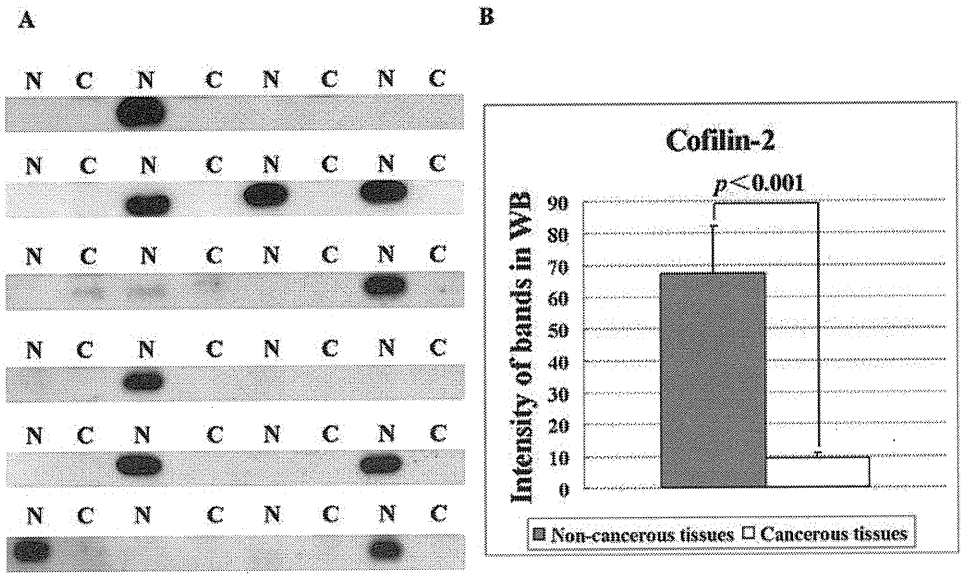

Figure 4. Western blot analysis of cofilin-2 was carried out in pancreatic cancerous and paired non-cancerous tissues. (A) Pancreatic cancerous (C) and paired non-cancerous (N) tissues from 24 PC patients were used, and the anti-cofilin-2 antibody was applied. The expression of cofilin-2 was barely detectable in the pancreatic non-cancerous tissues (58.3%) and in the cancerous tissues (100%). (B) Comparison of the intensity of the bands between cancerous and non-cancerous tissues by the Student's t-test (n=24, p<0.001). The relative standard errors (SE) of cancerous and non-cancerous tissue samples were 14.749 and 1.758, respectively.

detectable in the non-cancerous tissue samples (10/24; 41.7%), but was not in the cancerous tissues (0/24) (Fig. 4A).

Discussion

LIM domain kinase 1 (LIMK1) and cofilin are important regulators of actin cytoskeleton, and up-regulated actin cytoskeleton enhances tumor cell migration and invasion (13). The LIMK1-mediated cofilin pathway is directly related with mammary tumor invasion and migration (14). Cofilin was found to regulate cell protrusion and motility through the spatial interaction of lamellipodium and lamella (15). Epidermal growth factor (EGF)-induced phosphatidylinositol 4,5-bisphosphate (PIP2) was found to regulate membrane translocation of cofilin in carcinoma cells (16). In the present study, non-muscle cofilin (cofilin-1) was up-regulated in pancreatic cancerous tissues compared with non-cancerous tissues as determined by proteomic profiling. Notably, we demonstrated that expression of the muscle cofilin (cofilin-2), an isoform of cofilin-1, was completely disrupted in pancreatic cancerous tissues by Western blotting.

Cofilin-1, a small ubiquitous protein (~18.5 kDa), regulates actin dynamics through its ability to bind and sever actin filaments during cell migration (17). Cofilin-1 plays roles in cell proliferation, phagocytosis, chemotactic movement and macropinocytosis (18,19). It is generally regarded as an accessory to tumor cell invasion and motility (13). Inhibition of cofilin-1 activity in carcinoma cells reduces cell motility and invasion (20). Cofilin-1 expression was found to be up-regulated in many types of tumor cells, such as invasive mammary tumor cells (21), human glioblastoma cells (22) and the C6 rat glioblastoma cell line (23). In mammals, actin-depolymerizing factor (ADF)/cofilins are a family of monomeric and filamentous actin binding proteins, consisting of three members, cofilin-1, cofilin-2 and ADF (17,24). Cytoskeletal dynamics and cell motility in mammalian cells require ADF and cofilin-1 activity (20). Thus, cofilin-1 may be involved in motility and invasion of tumor cells in PC.

However, little is known about cofilin-2 in humans. Cofilin-2 accumulates at substrate adhesion sites where cofilin-1 is almost completely excluded (25); a significant increase in cofilin-2 expression was noted during the aggregation stage of cell development under conditions of starvation in *Dictyostelium* cells. However, cofilin-1 exhibited an opposing and concomitant action (25).

These findings indicate that cofilin-1 and cofilin-2 may play different roles in the dynamic reorganization of the actin architecture respectively, and cell development may involve the participation of cofilin-2 under conditions of starvation (25). Cofilin-2 expression in human skeletal muscle and the heart is different from its expression in various tissues in post-transcriptional splicing of mRNA (26). Albeit cofilin-2 gene transcript was detected in the human pancreas; we demonstrated that this protein was barely expressed in pancreatic cancerous tissues (100%). Notably, not all non-cancerous tissue samples exhibited a high level of cofilin-2 expression; approximately 41.7% of the non-cancerous tissues showed obviously detectable cofilin-2 expression. The mechanism by which this occurs is not clearly understood. Presumably cofilin-2 exists in non-cancerous tissues only under conditions of starvation at levels required to maintain cell development (25) or survival. Starvation-induced autophagy is a mechanism which promotes cell survival (27). However, it has yet to be revealed whether starvation-induced cell autophagy is related to cofilin-2 expression. However, the expression of cofilin-2 may not be required by well-nourished non-cancerous tissues in PC. Therefore, cofilin-2 may be related to the struggle between the body and tumors under conditions of starvation. Whether cofilin-2 is involved in resistance to starvation by a

self-regulating protective mechanism in non-cancerous tissue cells during PC progression must be clarified by further study.

The present study suggests that cofilin isoforms (cofilin-1/2) play essential roles in the destabilization of the actin cytoskeleton in PC progression involving different pathways. In order to clarify whether cofilin isoforms dysregulated in PC lead to rapid tumor spread, further investigations concerning their expression levels in PC cell lines and the determination of the effects of the cofilin pathways on invasion, proliferation or autophagy of these cells must be carried out. In addition, reports have demonstrated that cofilin expression is related to treatment resistance in PC cell lines (28,29). Therefore, our study indicates that cofilin isoforms may be useful clinical biomarkers or effective targets for controlling PC progression.

Acknowledgements

This study was supported in part by Grants-in-Aid from the Ministry of Health, Labour and Welfare of Japan (no. H20-Bio-005 to K.N.).

References

1. Jemal A, Siegel R, Ward E, Hao Y, Xu J and Thun MJ: Cancer statistics, 2009. CA Cancer J Clin 59: 225-249, 2009.
2. Kuramitsu Y, Miyamoto H, Tanaka T, Zhang X, Fujimoto M, Ueda K, Tanaka T, Hamano K and Nakamura K: Proteomic differential display analysis identified upregulated astrocytic phosphoprotein PEA-15 in human malignant pleural mesothelioma cell lines. Proteomics 9: 5078-5089, 2009.
3. Luk JM, Lam CT, Siu AF, Lam BY, Ng IO, Hu MY, Che CM and Fan ST: Proteomic profiling of hepatocellular carcinoma in Chinese cohort reveals heat-shock protein (Hsp27, Hsp70, GRP78) up-regulation and their associated prognostic values. Proteomics 6: 1049-1057, 2006.
4. Roth U, Razawi H, Hommer J, Engelmann K, Schwientek T, Müller S, Baldus SE, Patsos G, Corfield AP, Paraskeva C and Hanisch FG: Differential expression proteomics of human colorectal cancer based on a syngeneic cellular model for the progression of adenoma to carcinoma. Proteomics 10: 194-202, 2010.
5. Kuramitsu Y, Harada T, Takashima M, Yokoyama Y, Hidaka I, Iizuka N, Toda T, Fujimoto M, Zhang X, Sakaida I, Okita K, Oka M and Nakamura K: Increased expression and phosphorylation of liver glutamine synthetase in well-differentiated hepatocellular carcinoma tissues from patients infected with hepatitis C virus. Electrophoresis 27: 1651-1658, 2006.
6. Wang Y, Kuramitsu Y, Yoshino S, Takashima M, Zhang X, Ueno T, Suzuki N, Oka M and Nakamura K: Screening for serological biomarkers of pancreatic cancer by two-dimensional electrophoresis and liquid chromatography-tandem mass spectrometry. Oncol Rep 26: 287-292, 2011.
7. Tanaka T, Kuramitsu Y, Fujimoto M, Naito S, Oka M and Nakamura K: Downregulation of two isoforms of ubiquitin carboxyl-terminal hydrolase isozyme L1 correlates with high metastatic potentials of human SN12C renal cell carcinoma cell clones. Electrophoresis 29: 2651-2659, 2008.
8. Kuramitsu Y, Hayashi E, Okada F, Tanaka T, Zhang X, Ueyama Y and Nakamura K: Proteomic analysis for nuclear proteins related to tumour malignant progression: a comparative proteomic study between malignant progressive cells and regressive cells. Anticancer Res 30: 2093-2099, 2010.
9. Kuramitsu Y, Baron B, Yoshino S, Zhang X, Tanaka T, Yashiro M, Hirakawa K, Oka M and Nakamura K: Proteomic differential display analysis shows up-regulation of 14-3-3 protein sigma in human scirrhous-type gastric carcinoma cells. Anticancer Res 30: 4459-4465, 2010.
10. Kuramitsu Y, Taba K, Ryozawa S, Yoshida K, Tanaka T, Zhang X, Maehara S, Maehara Y, Sakaida I and Nakamura K: Identification of up- and down-regulated proteins in gemcitabine-resistant pancreatic cancer cells using two-dimensional gel electrophoresis and mass spectrometry. Anticancer Res 30: 3367-3372, 2010.
11. Kuramitsu Y, Hayashi E, Okada F, Zhang X, Tanaka T, Ueyama Y and Nakamura K: Staining with highly sensitive Coomassie brilliant blue SeePico™ stain after Flamingo™ fluorescent gel stain is useful for cancer proteomic analysis by means of two-dimensional gel electrophoresis. Anticancer Res 30: 4001-4005, 2010.
12. Mori-Iwamoto S, Kuramitsu Y, Ryozawa S, Mikuria K, Fujimoto M, Maehara S, Maehara Y, Okita K, Nakamura K and Sakaida I: Proteomics finding heat shock protein 27 as a biomarker for resistance of pancreatic cancer cells to gemcitabine. Int J Oncol 31: 1345-1350, 2007.
13. Yamaguchi H and Condeelis J: Regulation of the actin cytoskeleton in cancer cell migration and invasion. Biochim Biophys Acta 1773: 642-652, 2007.
14. Wang W, Mouneimne G, Sidani M, Wyckoff J, Chen X, Makris A, Goswami S, Bresnick AR and Condeelis JS: The activity status of cofilin is directly related to invasion, intravasation, and metastasis of mammary tumors. J Cell Biol 173: 395-404, 2006.
15. Delorme V, Machacek M, DerMardirossian C, Anderson KL, Wittmann T, Hanein D, Waterman-Storer C, Danuser G and Bokoch GM: Cofilin activity downstream of Pak1 regulates cell protrusion efficiency by organizing lamellipodium and lamella actin networks. Dev Cell 13: 646-662, 2007.
16. van Rheenen J, Song X, van Roosmalen W, Cammer M, Chen X, Desmarais V, Yip SC, Backer JM, Eddy RJ and Condeelis JS: EGF-induced PIP2 hydrolysis releases and activates cofilin locally in carcinoma cells. J Cell Biol 179: 1247-1259, 2007.
17. Bamburg JR: Proteins of the ADF/cofilin family: essential regulators of actin dynamics. Annu Rev Cell Dev Biol 15: 185-230, 1999.
18. Aizawa H, Sutoh K, Tsubuki S, Kawashima S, Ishii A and Yahara I: Identification, characterization, and intracellular distribution of cofilin in *Dictyostelium discoideum*. J Biol Chem 270: 10923-10932, 1995.
19. Aizawa H, Sutoh K and Yahara I: Overexpression of cofilin stimulates bundling of actin filaments, membrane ruffling, and cell movement in *Dictyostelium*. J Cell Biol 132: 335-344, 1996.
20. Hotulainen P, Paunola E, Vartiainen MK and Lappalainen P: Actin-depolymerizing factor and cofilin-1 play overlapping roles in promoting rapid F-actin depolymerization in mammalian nonmuscle cells. Mol Biol Cell 16: 649-664, 2005.
21. Wang W, Goswami S, Lapidus K, Wells AL, Wyckoff JB, Sahai E, Singer RH, Segall JE and Condeelis JS: Identification and testing of a gene expression signature of invasive carcinoma cells within primary mammary tumors. Cancer Res 64: 8585-8594, 2004.
22. Yap CT, Simpson TI, Pratt T, Price DJ and Maciver SK: The motility of glioblastoma tumour cells is modulated by intracellular cofilin expression in a concentration-dependent manner. Cell Motil Cytoskeleton 60: 153-165, 2005.
23. Gunnersen JM, Spirkoska V, Smith PE, Danks RA and Tan SS: Growth and migration markers of rat C6 glioma cells identified by serial analysis of gene expression. Glia 32: 146-154, 2000.
24. Vartiainen MK, Mustonen T, Mattila PK, Ojala PJ, Thesleff I, Partanen J and Lappalainen P: The three mouse actin-depolymerizing factor/cofilins evolved to fulfill cell-type-specific requirements for actin dynamics. Mol Biol Cell 13: 183-194, 2002.
25. Aizawa H, Kishi Y, Iida K, Sameshima M and Yahara I: Cofilin-2, a novel type of cofilin, is expressed specifically at aggregation stage of *Dictyostelium discoideum* development. Genes Cells 6: 913-921, 2001.
26. Thirion C, Stucka R, Mendel B, Gruhler A, Jaksch M, Nowak KJ, Binz N, Laing NG and Lochmüller H: Characterization of human muscle type cofilin (CFL2) in normal and regenerating muscle. Eur J Biochem 268: 3473-3482, 2001.
27. Codogno P: Autophagy in cell survival and death. J Soc Biol 199: 233-241, 2005.
28. Sinha P, Hütter G, Köttgen E, Dietel M, Schadendorf D and Lage H: Increased expression of epidermal fatty acid binding protein, cofilin, and 14-3-3-sigma (stratifin) detected by two-dimensional gel electrophoresis, mass spectrometry and microsequencing of drug-resistant human adenocarcinoma of the pancreas. Electrophoresis 20: 2952-2960, 1999.
29. Cecconi D, Astner H, Donadelli M, Palmieri M, Missiaglia E, Hamdan M, Scarpa A and Righetti PG: Proteomic analysis of pancreatic ductal carcinoma cells treated with 5-aza-2'-deoxycytidine. Electrophoresis 24: 4291-4303, 2003.

Proteomic Differential Display Analysis for TS-1-resistant and -sensitive Pancreatic Cancer Cells Using Two-dimensional Gel Electrophoresis and Mass Spectrometry

KANAKO YOSHIDA[1,2], YASUHIRO KURAMITSU[1], KOHEI MURAKAMI[1], SHOMEI RYOZAWA[2], KUMIKO TABA[1,2], SEIJI KAINO[2], XIULIAN ZHANG[1], ISAO SAKAIDA[2] and KAZUYUKI NAKAMURA[1]

Departments of [1]Biochemistry and Functional Proteomics, and [2]Gastroenterology and Hepatology, Yamaguchi University Graduate School of Medicine, 1-1-1 Minami-kogushi, Ube, Yamaguchi, Japan

Abstract. *TS-1 is an oral anticancer agent containing two biochemical modulators for 5-fluorouracil (5-FU) and tegafur (FT), a metabolically activated prodrug of 5-FU. TS-1 has been recognized as an effective anticancer drug using standard therapies for patients with advanced pancreatic cancer along with gemcitabine. However, a high level of inherent and acquired tumor resistance to TS-1 induces difficulty in the treatment. To identify proteins linked to the TS-1-resistance of pancreatic cancer, we profiled protein expression levels in samples of TS-1-resistant and -sensitive pancreatic cancer cell lines by using two-dimensional gel electrophoresis (2-DE) and liquid chromatography–tandem mass spectrometry (LC-MS/MS). The cytotoxicity of a 5-FU/5-chloro-2,4-dihydroxypyridine (CDHP) combination towards pancreatic cancer cell lines was evaluated by MTS assay. Panc-1, BxPC-3, MiaPaCa-2 and PK59 showed high sensitivity to the 5-FU/CDHP combination (TS-1-sensitive), whereas PK45p and KLM-1 were much less sensitive (TS-1-resistant). Proteomic analysis showed that eleven spots, including T-complex protein 1 subunit beta, ribonuclease inhibitor, elongation factor 1-delta, peroxiredoxin-2 and superoxide dismutase (Cu-Zn), appeared to be down-regulated, and 29 spots, including hypoxia up-regulated protein 1, lamin-A/C, endoplasmin, fascin and annexin A1, appeared to be up-regulated in TS-1-resistant cells compared with -sensitive cells. These results suggest that the identified proteins showing different expression between TS-1-sensitive and -resistant pancreatic cancer cells possibly relate to TS-1-sensitivity. These findings could be useful to overcome the TS-1-resistance of pancreatic cancer cells.*

Correspondence to: Yasuhiro Kuramitsu, MD, Ph.D., Department of Biochemistry and Functional proteomics, Yamaguchi University Graduate School of Medicine, 1-1-1 Minami-Kogushi, Ube, Yamaguchi 755-8505, Japan. Tel: +81 836222213, Fax: +81 836222212, e-mail: climates@yamaguchi-u.ac.jp

Key Words: Two-dimensional gel electrophoresis, LC-MS/MS, pancreatic cancer, TS-1, proteomics.

Pancreatic cancer is one of the most fatal types of cancer worldwide, and is the fifth leading cause of cancer death in Japan. The 5-year survival rate of this cancer is the lowest among patients with common types of cancer. Since pancreatic cancer invades progressively and metastasizes to liver and lymph nodes during early stages without remarkable symptoms, many patients have locally advanced or metastatic disease on presentation (1).

Gemcitabine and TS-1 are currently drugs of choice to treat patients with advanced pancreatic cancer. TS-1 is an oral fluoropyrimidine formulation that combines tegafur, 5-chloro-2,4-dihydroxypyridine (CDHP), and potassium oxonate at a molar ratio of 1:0.4:1 (2). The effect of TS-1 is expected to prolong survival of patients with advanced pancreatic cancer (3). However, TS-1-induced drug resistance of pancreatic cancer impacts its therapeutic effect. Thus, a better understanding of the molecular mechanisms of TS-1 resistance is essential to allow TS-1 to be used more effectively.

Proteomics is a powerful tool for identifying proteins whose expressions are different between drug-resistant and drug-sensitive cells. Proteomic differential display is a popular method to analyze protein expression profiling from two groups. Generally, two-dimensional gel electrophoresis (2-DE) and mass spectrometry (MS) have been used for this differential display method (4). Two-DE is able to separate proteins according to both their charge in isoelectoric focusing (IEF) gels and their weight in sodium dodecyl sulfate (SDS) gels. Two-DE has unique advantages for examining the expressions of hundreds of proteins simultaneously and for examining post-translational modifications of the protein spots. Our previous reports used proteomics and identified heat-shock protein 27 (HSP27) as a key molecule playing an important role in gemcitabine resistance (5-7).

0250-7005/2011 $2.00+.40

The aim of this study was to identify proteins showing differential expression in TS-1-resistant and -sensitive pancreatic cancer cell lines by using proteomics with 2-DE and liquid chromatography (LC)-MS/MS.

Materials and Methods

Tumor cell lines and culture conditions. All cell lines were obtained from Cell Resource Center for Biomedical Research Institute of Development, Aging and Cancer, Tohoku University. Two human pancreatic adenocarcinoma cell lines Panc-1 and MiaPaCa-2 were grown in Dulbecco's modified Eagle's medium with 4 mM L-glutamine adjusted to contain 1.5 g/l sodium bicarbonate, 4.5 g/l glucose and 10% fetal bovine serum. BxPC-3, KLM-1, PK45p and PK59 cells were grown in RPMI-1640 medium with 2 mM L-glutamine adjusted to contain 1.5 g/l sodium bicarbonate, 4.5 g/l glucose, 10 mM HEPES, 1.0 mM sodium pyruvate and 10% FBS. Cells were incubated in a humidified atmosphere containing 5% CO_2 at 37°C (6). All cell lines are not known to be TS-1-resistant or -sensitive.

Compounds. 5-Fluorouracil (5-FU) and a reversible competitive dihydropyrimidine dehydrogenase (DPD) inhibitor, 5-chloro-2,4-dihydrogenase (CDHP) were kindly provided by Taiho Inc. (Tokyo, Japan).

Effect of 5-FU/CDHP on proliferation of pancreatic cancer cells. Concentrations of 5-FU/CDHP which induced 50% cell death (IC_{50}) of each cell line were assessed by using 3-(4,5-dimethylthiazol-2-yl)-5-(3-carboxymethoxyphenyl)-2-(4-sulfophenyl)-2*H*-tetrazolium (MTS) (Promega Corp. Madison, WI, USA) assay, which is based on the reduction of this tetrazolium salt by viable cells. Briefly, cells (1×10^4 cells per well) were seeded in complete medium in 96-well plates, and cultured for 24 h. The 5-FU/CDHP mixture was used at a molar ratio of 1:1, which mimics human plasma pharmacokinetics after oral administration of TS-1(8). To determine the growth rate, cells in sextuplicate wells were mixed with 20 μL of MTS solution 72 h after 5-FU/CDHP exposure. After 3 h, the optical density of the dissolved material was measured at 490 nm with a microtiter plate reader (Model 550 Microplate Reader; Bio-Rad, Hercules, CA, USA). Results were derived from at least three independent sets of sextuplicate experiments.

Sample preparation. Cells were homogenized in lysis buffer (50 mM Tris-HCl, pH 7.5, 165 mM sodium chloride, 10 mM sodium fluoride, 1 mM sodium vanadate, 1 mM phenylmethylsulfonyl fluoride, 10 mM EDTA, 10 μg/ml aprotinin, 10 μg/ml leupeptin, and 1% NP-40) on ice. Suspensions were incubated for 1 h at 4°C, centrifuged at 21,500 ×*g* for 30 min at 4°C, and the supernatants were used as samples (9).

Two-dimensional gel electrophoresis (2-DE). The 2-DE consisted of IEF and SDS-polyacrylamide gel electrophoresis (SDS-PAGE). IEF was performed in an IPGphor 3 IEF unit (GE Healthcare, Buckinghamshire, UK) on 11 cm, immobilized, pH 3-10 linear gradient strips (Bio-Rad) at 50 μA/strip. SDS-PAGE was performed on a precast polyacrylamide gel with a linear concentration gradient of 5-20% (Bio-Rad), run at 200 V (10, 11).

Fluorescent gel staining. After 2-DE, the gels were washed with Milli-Q water three times, and fixed with 40% ethanol and 10% acetic acid for 4 h, and then stained with Flamingo™ Fluorescent Gel Stain (Bio-Rad) overnight. Stained gels were washed with Milli-Q water three times (12).

Image analysis and spot selection. Digitized images of the gels were acquired by scanning with a ProEXPRESS 2D Proteomic Imaging System (PerkinElmer Inc., Waltham, MA, USA). Image alignment, spot detection, background removal and expression analysis were performed by Progenesis SameSpot software (Nonlinear Dynamics Ltd. Newcastle upon Tyne, UK) (13). The differences in expression between TS-1-sensitive pancreatic cancer cell lines and TS-1-resistant pancreatic cancer cell lines were analyzed statistically by ANOVA test. 2-DE analysis was performed three times. After statistical analysis, the gels were re-stained with See Pico™ (Benebiosis Co., Ltd, Seoul, Korea) (14), and the selected spots whose expression was significantly different between TS-1-sensitive pancreatic cancer cell lines and TS-1-resistant pancreatic cancer cell lines were cut and removed for LC-MS/MS analysis.

LC-MS/MS. After in-gel digestion, protein samples were dissolved in 0.1% formic acid, centrifuged at 21,500×*g* for 5 min and the supernatant was used. An Agilent 1100 LC/MSD Trap XCT (Agilent Technologies, Palo Alto, CA, USA) was used for LC-MS/MS. Twenty-five microliters of each sample were applied and separated on a column (Zorbax 300SB-C18, 75 μm, 150 mm; Agilent Technologies). The Agilent 1100 capillary pump was operated under the following conditions: solvent A: 0.1% formic acid, solvent B: acetonitrile in 0.1% formic acid; column flow: 0.3 μl/min, primary flow: 300 μl/min; gradient: 0-5 min 2% solvent B, 60 min 60% solvent B; stop time: 60 min. Protein identification was performed in an Agilent Spectrum Mill MS proteomics workbench seeking MS/MS spectra using MS/MS ion search (15, 16) with the Swiss-Prot protein database search engine (http://kr.expasy.org/sprot/) and the MASCOT MS/MS Ions search engine (http://www.matrixscience.com/search_form_select.html). The criteria for positive identification of proteins were set as follows: filter by protein score >10.0, and filter peptide by score >8, % scored peak intensity (% SPI) >70.

Results

Selection of pancreatic cancer cell lines by TS-1 exposure. To evaluate the cytotoxicity of TS-1 in the pancreatic cancer cell lines, MiaPaCa-2, Panc-1, BxPC-3, PK45p and PK59 cells were exposed to different concentrations of the drug for 72 h. The 5-FU/CDHP mixture was used at a molar ratio of 1:1, which mimics human plasma pharmacokinetics after oral administration of TS-1. Based on the measurements obtained, the IC_{50} value was defined as the concentration of 5-FU/CDHP mixture causing 50% inhibition of growth. Four cell lines, Panc-1, BxPC-3, MiaPaCa-2 and PK59 showed a high sensitivity to 5-FU/CDHP mixture, with IC_{50} values of 33.4, 217.9, 250.8 and 330.5 μM, respectively. In contrast, PK45p and KLM-1 cells were much less sensitive; their IC_{50} values were 2087.0 and 3343.7 μM, respectively. The cell lines were thus classified into two groups: TS-1-sensitive cells (Panc-1, BxPC-3, MiaPaCa-2 and PK59) and TS-1-resistant cells (PK45p and KLM-1).